

# JGR Atmospheres

## RESEARCH ARTICLE

10.1029/2019JD030686

### Key Points:

- A copula-based probabilistic framework was proposed for conducting high-resolution projections of multivariate drought characteristics
- High-resolution climate projections were developed using the convection-permitting WRF model with the 4-km horizontal grid spacing
- A probabilistic multivariate drought index was introduced to examine joint effects of soil moisture and runoff deficits

### Supporting Information:

- Supporting Information S1

### Correspondence to:

S. Wang,  
shuo.s.wang@polyu.edu.hk

### Citation:

Zhang, B., Wang, S., & Wang, Y. (2019). Copula-based convection-permitting projections of future changes in multivariate drought characteristics. *Journal of Geophysical Research: Atmospheres*, 124, 7460–7483. <https://doi.org/10.1029/2019JD030686>

Received 21 MAR 2019

Accepted 18 JUN 2019

Accepted article online 24 JUN 2019

Published online 16 JUL 2019

### Author Contributions:

**Conceptualization:** S. Wang

**Data curation:** Y. Wang

**Formal analysis:** B. Zhang

**Funding acquisition:** S. Wang

**Investigation:** S. Wang

**Methodology:** B. Zhang, S. Wang

**Project administration:** S. Wang

**Resources:** S. Wang

**Software:** B. Zhang

**Supervision:** S. Wang



**Validation:** B. Zhang, Y. Wang

**Visualization:** B. Zhang, Y. Wang

**Writing - original draft:** B. Zhang

**Writing - review & editing:** S. Wang

## Copula-Based Convection-Permitting Projections of Future Changes in Multivariate Drought Characteristics

B. Zhang<sup>1</sup> , S. Wang<sup>1</sup> , and Y. Wang<sup>2</sup>

<sup>1</sup>Department of Land Surveying and Geo-Informatics, The Hong Kong Polytechnic University, Hong Kong, <sup>2</sup>Department of Geosciences, Texas Tech University, Lubbock, TX, USA

**Abstract** Probabilistic projections of future drought characteristics play a crucial role in climate change adaptation and disaster risk reduction. This study presents a copula-based probabilistic framework for projecting future changes in multivariate drought characteristics through convection-permitting Weather Research and Forecasting simulations with 4-km horizontal grid spacing. A probabilistic multivariate drought index is introduced to examine the joint effects of drought indicators with uncertainty intervals for four major river basins located in South Central Texas of the United States. Markov chain Monte Carlo is used to address uncertainties in assessing copula parameters and in predicting climate-induced changes in hydrological regimes. Our findings reveal that the severity and intensity of drought episodes can be amplified when considering the compound effects of soil moisture and runoff regimes by using the probabilistic multivariate drought index. The South Central Texas region is projected to experience more drought events with shorter duration and higher intensity in a changing climate. The drought severity will not necessarily increase due to the decreasing drought duration. In addition, our findings indicate that the intensity of future droughts is expected to increase as a result of the deficiency of soil moisture even though precipitation extremes are projected to become more frequent. Moreover, climate change impacts on multivariate drought characteristics will intensify with the increasing temporal scales (i.e., short-, medium-, and long-term droughts) although the number of future drought events may decrease by the end of this century.

**Plain Language Summary** Projecting future changes in drought characteristics plays a crucial role in climate change adaptation and disaster risk reduction. Here we present a copula-based probabilistic framework for conducting high-resolution projections of multivariate drought characteristics through convection-permitting Weather Research and Forecasting simulations with the 4-km horizontal grid spacing. A probabilistic multivariate drought index is also introduced to examine the joint effects of drought indicators for four major river basins located in South Central Texas of the United States. Our findings reveal that the severity and intensity of drought episodes can be amplified when considering the compound effects of soil moisture and runoff regimes. Furthermore, the long-lasting droughts are expected to evolve into a series of short-duration droughts due to the projected increase in the frequency and intensity of extreme precipitation in a changing climate. This study provides meaningful insights into the evolution of future drought characteristics in view of the increasing trend in extreme precipitation, which plays an important role in facilitating sustainable agricultural development and water resources planning under climate change.

## 1. Introduction

Drought is a recurrent natural disaster characterized by a prolonged period of water deficit. Many countries have experienced severe drought events over the past decade, inflicting catastrophic economic ramifications, severe ecological damages, food shortages, and millions of deaths (AghaKouchak et al., 2014). In 2012, for example, the United States suffered from the heaviest drought since 1956, causing a direct economic loss of over \$35 billion in the Midwest and a huge indirect effect on global food security (Pozzi et al., 2013). Mounting evidence suggests that global warming is an indisputable fact, which confronts all mankind with an urgent question: How severe will future droughts be under climate change? This question has attracted increasing attention from all over the world in recent years since it is crucial for enhancing resilience to climate-induced disasters and for developing sound climate change mitigation and adaptation strategies

(Carvalho & Wang, 2019; Pozzi et al., 2013; Prudhomme et al., 2014; Rajsekhar et al., 2015a; Su et al., 2018; Wan et al., 2017; Wang et al., 2011).

Quantification of droughts is the prerequisite for analyzing climate change impacts on future droughts. Droughts are typically categorized into four classes: meteorological, agricultural, hydrological, and socio-economical droughts. Meteorological drought is characterized by the precipitation deficit, while the main feature of agricultural drought is a lack of soil moisture that is the direct source of water for crop growth. Hydrological drought, on the other hand, is identified as a shortage of streamflow and groundwater supplies. Socio-economical drought refers to conditions where the water supply cannot satisfy the demand of various water-use sectors. Various indices have been proposed to quantify the four types of droughts in recent decades. For example, the standardized precipitation index (SPI) was proposed by McKee et al. (1993) to characterize the meteorological drought. Based on the concept of SPI, standardized soil moisture index (SSI, AghaKouchak, 2014) and standardized runoff index (SRI, Mo, 2008) were also widely used to monitor agricultural and hydrological droughts, respectively.

General circulation models (GCMs) are scientifically the most sophisticated approach to project future hydroclimatic information, which is useful for examining future changes in drought characteristics. Numerous studies based on GCMs have been conducted in recent decades to project future droughts at global, regional, or local scales (Zarch et al., 2015). For example, Wehner et al. (2011) indicated a projected increase in future drought frequency and severity over North America based on 19 state-of-the-art GCMs and Palmer drought severity index. Van Huijgevoort et al. (2014) disclosed that the future hydrological drought was expected to intensify based on three GCMs and five large-scale hydrological models. Ruosteenoja et al. (2018) found that the near-surface soil moisture content was projected to decrease in Europe for the 21st century based on 26 GCMs. However, recent studies have revealed that enormous uncertainties exist in the representation of droughts using GCMs (Johnson & Sharma, 2015; Moon et al., 2018; Zhu et al., 2019). This is because the spatial resolution of GCMs is too coarse to depict the heterogeneous climate patterns (e.g., clouds and convection processes) and extremes (e.g., extreme precipitation and temperature) at regional and local scales, particularly in mountainous regions, urban, and coastal areas.

Given the drawbacks of GCMs in drought projections, considerable efforts have been made to conduct dynamical downscaling simulations using regional climate models (RCMs, Leng et al., 2015; Prudhomme et al., 2014; Wang et al., 2011; Zhu et al., 2018). For example, Russo et al. (2013) utilized SPI to analyze climate change impacts on meteorological droughts based on the outputs from GCMs and RCMs. Rajsekhar and Gorelick (2017) found an increasing trend of droughts in Jordan based on bias-corrected RCMs and high-resolution hydrologic models. These regional climate studies, however, have their limitations. Typically, dynamical downscaling from coarse-resolution GCMs (e.g., over 200 km) to higher-resolution RCMs (e.g., 10–50 km) was conducted in these studies. Such RCMs are not fine enough to explicitly resolve deep convection, which is a particularly critical subgrid process operated at scales from the microscale to the synoptic scale. Convection parameterization schemes were thus used in RCMs to represent deep convection. Previous studies have shown that common errors and uncertainties inherently exist in climate simulations through RCMs with convection parameterization schemes (Berg et al., 2013; Prein et al., 2013). For example, the convection parameterization schemes misrepresent convective precipitation, leading to an underestimation of dry days and overestimation of low-precipitation event frequency (Brockhaus et al., 2008). Furthermore, precipitation is the primary driving forcing of hydrological models; the outputs of RCMs are thus particularly unreliable for hydrological drought projections. Consequently, it is desired to conduct high-resolution climate simulations (horizontal grid spacing  $\leq 4$  km) that can explicitly resolve convection processes without the use of parameterization schemes, improving robustness and reliability of drought projections. On the other hand, probabilistic hydrological predictions have been proven by the hydrologic community to be superior to deterministic predictions due to various sources of uncertainty (e.g., uncertainties in model parameters and inputs, Wang et al., 2018). Previous studies based on deterministic hydrological predictions may lead to a biased hydrological drought projection. It is thus necessary to develop probabilistic hydrological drought projections for improving reliability of drought analysis.

The drought phenomenon involves a series of complicated and interactive physical processes. Numerous studies have shown that drought characterization based on a single variable (or indicator) is unreliable (Kang & Sridhar, 2017; Rajsekhar & Gorelick, 2017; Wang et al., 2011). Thus, a variety of methods have

been utilized to examine the joint effects of drought indicators in order to perform a comprehensive drought assessment. These methods mainly include copula (Kao & Govindaraju, 2010), linear combination (Xia et al., 2014), principal component analysis (Keyantash & Dracup, 2004), fuzzy set (Huang et al., 2015), and entropy theory (Rajsekhar et al., 2015b). Copulas have emerged as a widely used approach due to its capability of capturing complicated dependencies between various drought variables (Hao & AghaKouchak, 2013; Kang & Sridhar, 2017). These copula-based multivariate drought assessments, however, neglect the underlying uncertainties of copula parameters. And the copula parameters are commonly estimated by local optimization methods, which are often biased because of getting trapped in local minima (Genest et al., 2009; Kwon & Lall, 2016). In addition, Sadegh et al. (2017) revealed that significant uncertainties existed in copula parameters, especially for those cases with a limited length of data. Thus, uncertainties in the copula-based multivariate drought assessment should be addressed to enhance robustness in future drought projections.

In this study, we will develop copula-based probabilistic projections of multivariate drought characteristics through convection-permitting (Weather Research and Forecasting, WRF) simulations. Specifically, a copula-based probabilistic multivariate drought index (PMDI) will be introduced to examine the joint effects of soil moisture deficit (agricultural drought) and runoff deficit (hydrological drought). The Markov chain Monte Carlo (MCMC) simulations will be performed to address uncertainties in copula parameters and hydrological model parameters, leading to probabilistic projections of multivariate drought characteristics. Future changes in drought episodes will be projected for four major river basins located in South Central Texas of the United States, which is the primary concern of the Texas Department of Agriculture and the Texas Water Development Board. The Parameter-elevation Regressions on Independent Slopes Model (PRISM) data set will be utilized to verify the WRF simulations. The Model Parameter Estimation Experiment (MOPEX) data set and the data collected from the United States Geological Survey river flow gauging stations will be used to calibrate and validate the hydrological model.

This paper will be organized as follows. Section 2 will describe the copula-based probabilistic framework of multivariate drought projections, models, algorithms, and data sets used in this study. Section 3 will provide an assessment of the PMDI performance, a high-resolution projection of future changes in climate variables and runoff regimes, and an investigation of climate change impacts on multivariate drought characteristics of different temporal scales. The contribution of uncertainties in copula and hydrological model parameters to the overall uncertainty in multivariate drought projections will also be discussed. Finally, conclusions and findings of this study will be drawn in section 4.

## 2. Models, Algorithms, and Data Sources

### 2.1. A Copula-Based Probabilistic Framework of Multivariate Drought Projections

To conduct a reliable and robust projection of multivariate drought characteristics, we propose a copula-based probabilistic framework, as shown in Figure 1. The first step is to collect the data including the PRISM, the National Centers for Environmental Prediction (NCEP) Climate Forecast System Reanalysis (CFSR), and the MOPEX data sets. Details of data sources are given in section 2.7. The second step is to construct the copula-based PMDI. The uncertainty in copula parameters will be addressed using the MCMC algorithm. The detailed descriptions of the PMDI and the MCMC algorithm are provided in sections 2.2 and 2.6, respectively. PMDI will be compared against SSI and SRI based on historical observations to assess its performance. In addition, the drought duration, severity, and intensity will be quantified based on the run theory that has been extensively used to quantify drought characteristics (Leng et al., 2015; Rajsekhar & Gorelick, 2017; Wang et al., 2011; Yevjevich, 1967). Details of the multivariate drought characterization are illustrated in section 2.3. The third step is to conduct and evaluate the convection-permitting climate simulations, as described in section 2.4. The fourth step is to carry out the MCMC-based hydrological simulations that are validated against streamflow observations from the United States Geological Survey river flow gauging stations. The detailed description of the hydrological modeling is provided in section 2.5. The fifth step is to project future changes in multivariate drought characteristics for four major river basins located in South Central Texas of the United States. The probabilistic runoff time series will be predicted based on the outputs of the convection-permitting climate projections. The copula-based PMDI will then be used to calculate the cumulative joint probability of soil moisture and runoff regimes, leading to

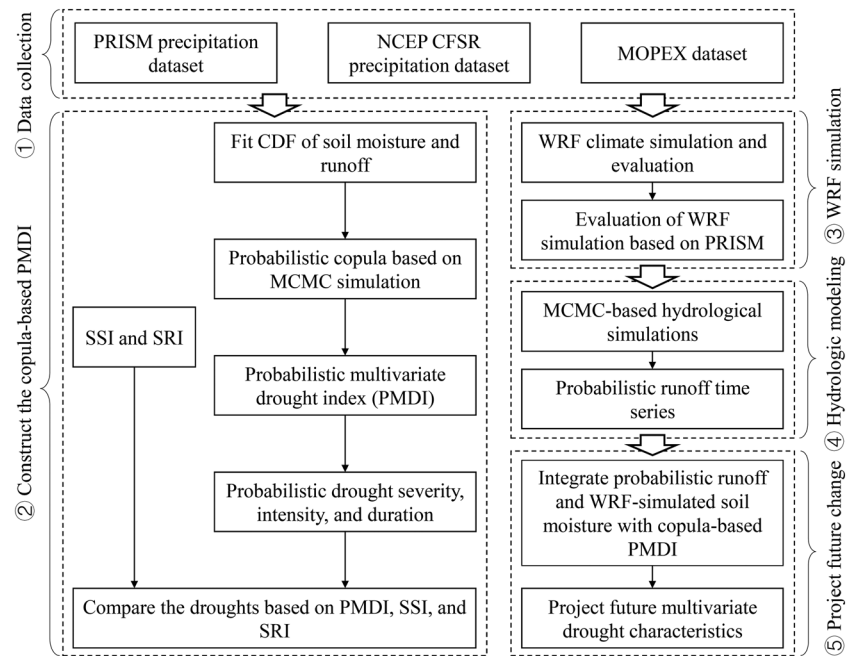


**Figure 1.** Flowchart of the copula-based probabilistic framework for conducting high-resolution projections of multivariate drought characteristics. NCEP = National Centers for Environmental Prediction; CFSR = Climate Forecast System Reanalysis; MOPEX = Model Parameter Estimation Experiment; CDF = cumulative distribution function; WRF = Weather Research and Forecasting; PRISM = Parameter-elevation Regressions on Independent Slopes Model; MCMC = Markov chain Monte Carlo; SSI = standardized soil moisture index; SRI = standardized runoff index.

probabilistic multivariate drought assessments. Details of all components involved within the developed computational framework are provided as follows.

## 2.2. Copula-Based PMDI

Copulas are mathematical functions that can be used to derive the joint distribution of two or more random variables. In hydrological and climatological studies, the copula has been widely used to model the dependence between hydroclimatic variables. In recent years, copulas have also been used to develop multivariate drought indices by constructing the joint distribution of two or more hydroclimatic variables related to droughts, such as multivariate standardized drought index (MSDI) and standardized precipitation-streamflow index (Hao & AghaKouchak, 2013; Rad et al., 2017). In this study, a multivariate drought index (MDI) is introduced using copulas to examine the joint effect of soil moisture and runoff on drought characteristics. Given that soil moisture and runoff are expressed, respectively, as random variables  $X$  and  $Y$ , their cumulative joint probability  $p$  can be written as

$$P(X \leq x, Y \leq y) = C[F(X), G(Y)] = p \quad (1)$$

where  $C$  is the copula function.  $F(X)$  and  $G(Y)$  are the marginal cumulative distribution function (CDF) of  $X$  and  $Y$ , respectively. A variety of copula families have been proposed to model the dependence structures of random variables. For example, the Gumbel copula can be expressed as

$$C(u, v) = \exp \left\{ - \left[ (-\ln(u))^\theta + (-\ln(v))^\theta \right]^{1/\theta} \right\} \quad (2)$$

where  $\theta$  is the copula parameter.  $u$  and  $v$  are the marginal probabilities of soil moisture and runoff, respectively. The MDI used to model the dependence between soil moisture and runoff can then be defined by

$$\text{MDI} = \varphi^{-1}(p) \quad (3)$$

where  $\varphi$  is the standard normal distribution function. The joint probability  $p$  can be converted to the MDI using equation (3). Specifically, the first step is to construct the marginal distributions of soil moisture and

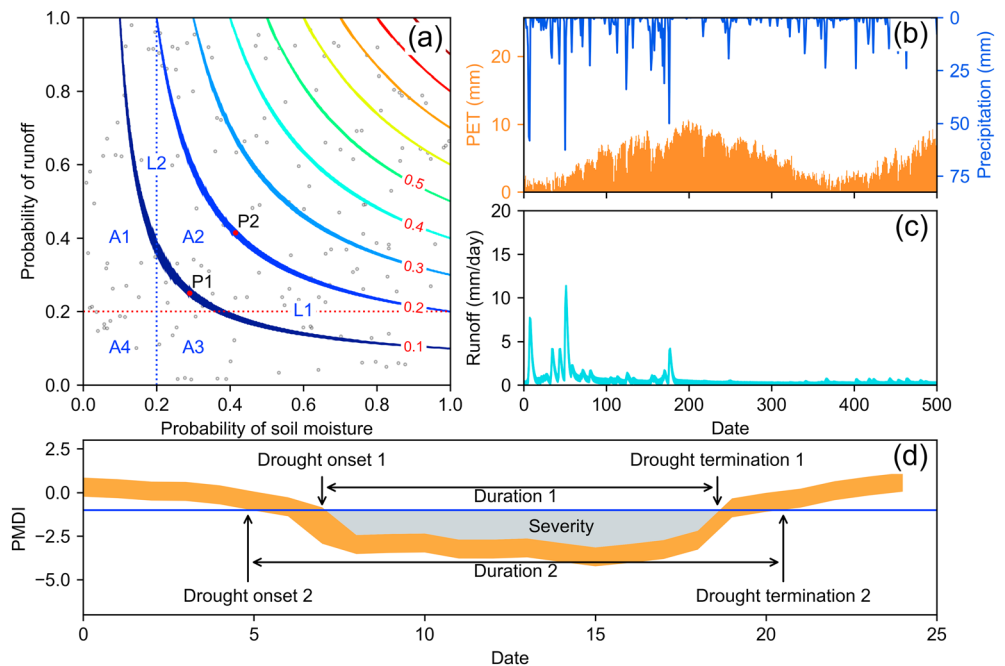


**Figure 2.** Schematic of probabilistic multivariate drought projections. (a) Probabilistic contours of joint cumulative distribution functions (CDFs) of soil moisture and runoff regimes. (b) Potential evapotranspiration (PET) and precipitation. (c) Probabilistic hydrologic predictions. (d) Multivariate drought characteristics with uncertainty intervals. The blue line represents the threshold used to identify drought events ( $-0.8$  was used in this study). PMDI = probabilistic multivariate drought index.

runoff. Runoff was collected from the U.S. MOPEX data set in this study, while soil moisture was obtained from the WRF simulation as an alternative since the long-term observations of soil moisture were unavailable. A total of 16 types of probability distributions, including Birnbaum-Saunders, exponential, extreme value, gamma, generalized extreme value, generalized Pareto, inverse Gaussian, logistic, loglogistic, lognormal, Nakagami, normal, Rayleigh, Rician,  $t$  location scale, and Weibull were used to fit soil moisture and runoff data. The optimal parameters for these probability distributions were obtained through the maximum likelihood estimation. The Akaike information criterion (AIC), the Bayesian information criterion (BIC), and the AIC with a correction for finite sample sizes (AICc) were used to evaluate the goodness of fit of each theoretical distribution. These evaluation criteria are defined as follows:

$$\text{AIC} = 2k - 2l \quad (4)$$

$$\text{BIC} = k \ln n - 2l \quad (5)$$

$$\text{AICc} = \text{AIC} + \frac{2k(k+1)}{n-k-1} \quad (6)$$

where  $k$  is the number of parameters of the probability distributions;  $l$  is the maximum log-likelihood value of the best parameter set based on the maximum likelihood estimation; and  $n$  is the number of observations. Note that the lower the values of AIC, BIC, and AICc, the better the copula model.

The next step is to identify the optimal copula model in order to well represent the structure of dependence between soil moisture and runoff. A variety of copula families have been developed to model the dependence structure of two or more random variables. Among these copula families, the Frank copula is commonly used to model symmetric dependence structures, while the Gumbel and Clayton copulas can be used to characterize asymmetric dependence structures. These three copula families have been widely used in hydrological and climatological literatures, and thus, they are selected in this study to model the theoretical dependence between soil moisture and runoff. To estimate copula parameters such as  $\theta$  in equation (2), the MCMC algorithm was used to derive the posterior parameter distributions, thereby leading to copula probability isolines with uncertainty intervals (Figure 2a). The MCMC-based copulas improve upon the



commonly used deterministic copulas by tackling the inherent uncertainty in copula parameters, leading to PMDI that can be used to characterize the dependence between soil moisture and runoff under uncertainty. The optimal copula family can be identified according to AIC, BIC, the root-mean-square error (RMSE), and the Nash-Sutcliffe efficiency (NSE). RMSE and NSE are defined as follows:

$$\text{RMSE} = \sqrt{\frac{\sum (X-Y)^2}{n}} \quad (7)$$

$$\text{NSE} = 1 - \frac{\sum (X-Y)^2}{\sum (Y-\bar{Y})^2} \quad (8)$$

where  $X$  and  $Y$  are the theoretical and empirical cumulative probability of random variables (soil moisture and runoff), respectively;  $n$  is the number of observations. The lower the RMSE and the closer to 1 the NSE, the more reliable the estimate.

### 2.3. Multivariate Drought Characterization With Uncertainty Intervals

The introduced PMDI can be used to perform the multivariate assessment of droughts relative to a climatological base period, including the agricultural drought associated with the lack of soil moisture and the hydrological drought associated with the lack of water supply as well as their interactions. Figure 2a shows the copula probability isolines derived using the PMDI. Assume that a given drought threshold of 20th percentile runoff and soil moisture was used to identify drought events (see dashed lines L1 and L2 of Figure 2a). As a result, all points within areas A1–A4 can be characterized as multivariate drought events including agricultural and hydrological droughts. Compared to existing multivariate drought indices such as MSDI and standardized precipitation-streamflow index, PMDI has the advantage of quantifying uncertainties inherent in the drought assessment and projection, thereby improving the ability of disaster management and risk assessment. For example, points P1 and P2 fall within the ranges of uncertainty intervals on the contours of the bivariate joint CDF, as shown in Figure 2a. The joint CDF values of P1 can be considered to be larger or smaller than 0.1 due to the uncertainty in copula parameters, which represents a moderate or a severe drought event, respectively. Moreover, P2 can be considered as a drought event or not since the joint CDF values of P2 can be considered to be smaller or larger than 0.2 under uncertainty. Thus, such uncertainties need to be taken into account for enhancing reliability and robustness of multivariate drought assessments.

When the probabilistic copula model is constructed, PMDI can be calculated according to equation (3). As shown in Figure 2d, PMDI exhibits with an uncertainty interval owing to the uncertainty in copula parameters. A drought event is typically identified as a period when the drought index remains consecutively below a threshold (e.g.,  $-0.84$  for MSDI). A threshold of  $-0.8$  was used in this study. As shown in Figure 2d, a drought event occurs when the value of PMDI is smaller than  $-0.8$ . The duration ( $D$ ), severity ( $S$ ), and intensity ( $I$ ) of the drought event are defined as

$$S = \sum_{i=1}^D -(\text{PMDI}_i + 1) \quad (9)$$

$$I = S/D \quad (10)$$

where  $i = 1$  is the start of a drought event when the value of PMDI drops below  $-0.8$  consecutively;  $D$  is the total duration from the onset to the drought termination (as shown in Figure 2d);  $S$  is the drought severity defined as the total sum of the difference between PMDI values and the threshold (i.e.,  $-0.8$ );  $I$  is the drought intensity which is the ratio of the drought severity ( $S$ ) to the drought duration ( $D$ ).

The characterization of drought properties in previous studies is derived from deterministic drought indices. The introduced copula-based PMDI enables multivariate drought characterization with uncertainty intervals, leading to probabilistic assessments and projections of drought characteristics including duration, severity, and intensity. For example, the upper and the lower bounds of the uncertainty interval (as shown in Figure 2d) represent two scenarios of a drought event: the best-case scenario and the worst-case scenario. For the best-case scenario, the gray area represents the drought severity; for the worst-case scenario, the drought severity is represented by the sum of the gray area and the orange area below the threshold of

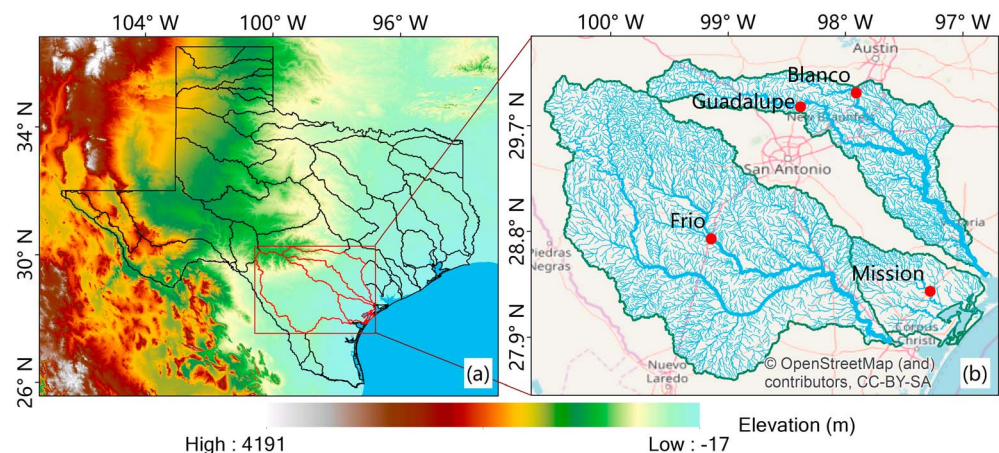


**Figure 3.** (a) Model domain with topography and (b) four major river basins including Guadalupe, Blanco, Mission, and Frio river basins over South Central Texas. The red points represent the location of USGS gauging stations with long-term precipitation, PET, and streamflow records. USGS = United States Geological Survey.

−0.8. It can be seen that the drought onset for the worst-case scenario is over 2 months earlier than that for the best-case scenario, which provides meaningful insights into proactive hazard preparedness and future planning. The drought duration for the worse-case scenario is thus over 4 months longer than that under the best-case scenario. Consequently, the worst-case scenario amplifies the severity and duration of a drought event, which should be taken into account for drought risk assessments. On the other hand, projecting future changes in drought characteristics incorporates climate simulations and hydrological predictions into a general computational framework, which brings more sources of uncertainty in multivariate drought analysis. For example, the potential evapotranspiration (PET) and precipitation obtained from the WRF simulations (Figure 2b) were used to perform the MCMC-based hydrological simulations in this study, leading to probabilistic predictions of runoff time series (Figure 2c). The probabilistic runoff time series was then utilized to conduct copula-based multivariate drought projections, leading to the dual uncertainty (i.e., two levels of uncertainty) including uncertainties in copula model and hydrological model parameters. The dual uncertainty further increases the difference between the best- and worse-case scenarios of multivariate droughts. It is thus necessary to address uncertainties inherent in the projections of multivariate drought characteristics through a thorough analysis of best- and worst-case scenarios, which improves the reliability and robustness of assessing climate change impacts on future droughts.

#### 2.4. Convection-Permitting Climate Modeling

The WRF model v3.7.1 was used in this study to conduct the convection-permitting climate simulations over Texas (Figure 3a). The model was operated at a region of  $1,520 \times 1,400$  km ( $380 \times 350$  grid points) with 51 stretched vertical levels topped at 50 hPa. The model domain has a 4-km horizontal grid spacing, which is fine enough to permit convective processes and well capture the details of the terrain. Thus, convection parameterization is not required for performing the 4-km WRF simulations. The NCEP CFSR data set was collected as the initial and lateral boundary conditions. This data set has a 6-hourly temporal resolution and a  $0.5^\circ \times 0.5^\circ$  spatial resolution. The historical climate simulation spans a 15-year period of 1981–1995. The model was configured with the Thompson cloud microphysics scheme, the Yonsei University planetary boundary layer scheme, the revised Monin-Obukhov surface layer scheme, and the Rapid Radiative Transfer Model shortwave and longwave radiation scheme. The land surface was simulated using the Noah-MP land surface scheme. The WRF simulations were compared against the PRISM data set to demonstrate model performance.

The high-resolution (4 km) climate projections were forced with the CFSR data, and the initial and boundary conditions were consecutively perturbed by using the pseudoglobal warming technique (Lauer et al., 2013; Liu et al., 2017; Wang & Wang, 2019). The perturbed physical fields include temperature, specific humidity, geopotential, sea surface temperature, horizontal wind, soil temperature, sea level pressure, and sea ice.

However, the sea ice was not perturbed in this study because there was no sea ice in the model domain. The climate perturbation was estimated through a 30-year multimodel ensemble mean climate change signal, as shown in equation (11). The historical and future climate projections were produced from the Coupled Model Intercomparison Project Phase 5 (CMIP5) under the Representative Concentration Pathway (RCP) 8.5 emission scenario.

$$\text{WRF}_{\text{input}} = \text{CFSR} + (\text{CMIP5}_{2071-2100} - \text{CMIP5}_{1976-2005}) \quad (11)$$

To minimize the influence of model uncertainties in quantifying the climate response to future greenhouse gas forcing, we used a multimodel ensemble mean climate difference between past and future periods. A total of 15 CMIP5 GCMs were selected based on their performance in simulating the climate over North America. Details of these 15 GCMs including their atmospheric grid spacing are provided in Table S1 of the supporting information. The CFSR reanalysis data were perturbed every 6 hr by the derived climate change signal in order to provide the WRF model with initial and boundary conditions for future climate projections.

### 2.5. Rainfall-Runoff Modeling

To assess climate change impacts on multivariate drought characteristics, the conceptual hydrological model (Hymod) was used to predict daily streamflow in four major river basins located in South Central Texas of the United States (Figure 3b). The daily streamflow was predicted based on the projected changes of precipitation and PET through the convection-permitting WRF simulations. PET is the maximum amount of water that would be evapotranspired if water availability were unlimited, which is calculated using the FAO-56 Penman-Monteith equation based on four climate variables including relative humidity, wind speed, solar radiation, and air temperature (Allen et al., 1998).

The Hymod is a parsimonious rainfall-runoff model based on the probability-distributed model (Moore, 2007), which has been widely used to perform uncertainty assessment of hydrological predictions for many river basins around the world (Herman et al., 2013; Roy et al., 2017; Sadegh & Vrugt, 2013; Wang et al., 2015). The Hymod consists of two modules, including a soil moisture accounting module and a routing module. The soil moisture accounting module is built based on the probability-distributed soil storage capacity principle introduced by Moore (1985). The distribution function of storage capacity is calculated by

$$F(C) = 1 - \left(1 - \frac{C}{C_{\max}}\right)^{b_{\exp}}, \quad 0 \leq C \leq C_{\max} \quad (12)$$

where  $C_{\max}$  denotes the maximum soil moisture storage capacity within the river basin, and  $b_{\exp}$  is a coefficient governing the nonlinearity of the storage capacity. In the Hymod, parameter  $\beta$  divides the soil overflow into quick- and slow-flow routing. The quick-flow routing includes a Nash cascade of three tanks, while the slow-flow routing contains only a single tank. The quick- and slow-flow processes are controlled by rate constants  $R_q$  and  $R_s$ , respectively. The simulated streamflow is the sum of quick and slow flow. Thus, the Hymod has five model parameters, including  $C_{\max}$ ,  $b_{\exp}$ ,  $\beta$ ,  $R_s$ , and  $R_q$ . More detailed descriptions on the Hymod can be seen at Moore (2007). Since the five parameters cannot be estimated with certainty, an uncertainty range was initially given for each parameter (see Table S2 of the supporting information).

### 2.6. MCMC Simulation

The MCMC algorithm has been recognized as an effective tool used to address uncertainties in model parameters within a Bayesian framework. Assume that  $\tilde{Y}$ ,  $X$ , and  $\theta$  signify a discrete vector of measurements, the forcing variables, and the unknown model parameters, respectively. By using a Bayesian formalism, the posterior distribution of model parameters can be derived by

$$p(\theta|\tilde{Y}) = \frac{p(\theta)p(\tilde{Y}|\theta)}{p(\tilde{Y})} \quad (13)$$

where  $p(\theta)$  and  $p(\theta|\tilde{Y})$  denote prior and posterior distributions of model parameters, respectively, and  $p(\tilde{Y}|\theta) \propto L(\theta|\tilde{Y})$  denotes the likelihood function.  $p(\tilde{Y})$  is the evidence that acts as a normalization



constant, which is not required for the posterior estimation in practice. Thus, equation (13) can be rewritten as

$$p(\theta|\tilde{Y}) \propto p(\theta)L(\theta|\tilde{Y}) \quad (14)$$

where  $L(\theta|\tilde{Y})$  is the likelihood function that represents the distance between model simulations and observations. Assume that the error residuals are uncorrelated and normally distributed, the likelihood function becomes

$$L(\theta|\tilde{Y}) = \prod_{t=1}^n \frac{1}{\sqrt{2\pi\tilde{\sigma}^2}} \exp \left[ -\frac{1}{2} \left( \frac{\tilde{y}_t - y_t(\theta)}{\tilde{\sigma}_t} \right)^2 \right] \quad (15)$$

where  $\tilde{\sigma}$  is the estimated standard deviation of the measurement error,  $\tilde{y}_t$  and  $y_t(\theta)$  are the observation at time  $t$  and the model simulation given parameter  $\theta$  at time  $t$ . For simplicity and numerical stability, equation (15) can be logarithmically transformed to

$$L(\theta|\tilde{Y}) = -\frac{n}{2} \log(2\pi) - \sum_{t=1}^n \{ \log(\tilde{\sigma}_t) \} - \frac{1}{2} \sum_{t=1}^n \left( \frac{\tilde{y}_t - y_t(\theta)}{\tilde{\sigma}_t} \right)^2 \quad (16)$$

Once the prior distribution and the likelihood function are specified, the Monte Carlo method is used to generate a sample of posterior distributions of model parameters.

The MCMC algorithm was developed based on a Markov chain that generated a random walk through the search space with the stable frequency stemming from a fixed probability distribution until the convergence to a stationary posterior distribution (Sadegh et al., 2017; Vrugt, 2016; Vrugt et al., 2008). In this study, the MCMC algorithm was used to address uncertainties in copula parameters and hydrological model parameters, leading to probabilistic projections of multivariate drought characteristics.

## 2.7. Data Sources

The PRISM data set was used to evaluate historical WRF simulations over Texas. The PRISM data set is a gridded data set with a  $4 \times 4$ -km grid resolution, which was produced using the *terrain-aware* interpolation techniques based on a number of gauge observations. In addition, the MOPEX data set was used to calibrate and validate hydrological simulations as well as to assess historical hydrological droughts based on SRI. A total of 15 years of daily streamflow from January 1981 to December 1995 was collected for each of the four major basins including Guadalupe, Blanco, Mission, and Frio river basins located in South Central Texas (Figure 3b). Due to the lack of long-term observations of soil moisture, the WRF-simulated soil moisture was used to assess historical agricultural droughts based on SSI. The soil moisture was averaged over the neighboring window of size  $3 \times 3$  centered at each MOPEX station in order to eliminate the bias caused by the spatially heterogeneous surface. The monthly MOPEX streamflow and the monthly WRF-simulated soil moisture were used together to conduct the multivariate assessment of droughts including hydrological and agricultural droughts over South Central Texas.

When hydrological model simulations were calibrated based on the MOPEX observations for the 10-year period from January 1981 to December 1990 and then validated for the 5-year period from January 1991 to December 1995, daily streamflow was predicted for each of the four Texas major river basins over the period from January 2085 to December 2099 based on the projected future changes in precipitation and PET derived from the WRF simulations. Different temporal scales (i.e., 3-, 6-, and 12-month) streamflow and soil moisture were then utilized to examine the projected changes in future multivariate drought characteristics.

## 3. Results and Discussion

### 3.1. Probabilistic Construction of Copulas

In this study, a total of 16 types of probability distributions were used to fit the theoretical CDF of soil moisture and runoff, and then the optimal CDF was chosen according to the derived values of AIC, BIC, and AICc. Figures 4 and 5 present the comparison between the empirical CDF and the theoretical CDF for 3-, 6-, and

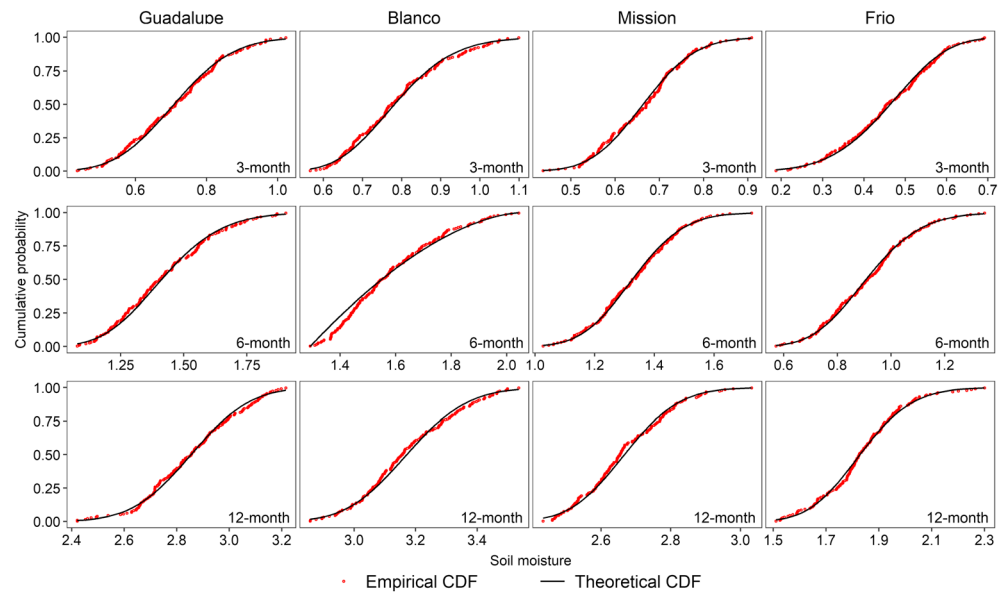


**Figure 4.** Comparison between the empirical CDFs and the theoretical CDFs for 3-, 6-, and 12-month soil moisture. The red points denote the empirical CDF, while the black lines denote the fitted optimal theoretical CDF. CDF = cumulative distribution function.

12-month soil moisture and runoff in the four river basins. Overall, there is a good agreement between the theoretical CDF and the empirical CDF across different temporal scales. The marginal posterior distributions of copula parameters estimated using the MCMC algorithm are well approximated by normal distributions (see Figure S1 of the supporting information).

By using the posterior distributions of copula parameters, the probabilistic joint CDF can be constructed to represent the dependence between soil moisture and runoff across different temporal scales for the four river basins (Figure 6). The results of goodness-of-fit tests for copulas are shown in Table S3 of the supporting information. It is indicated that the theoretical copulas can be used to well characterize the dependence

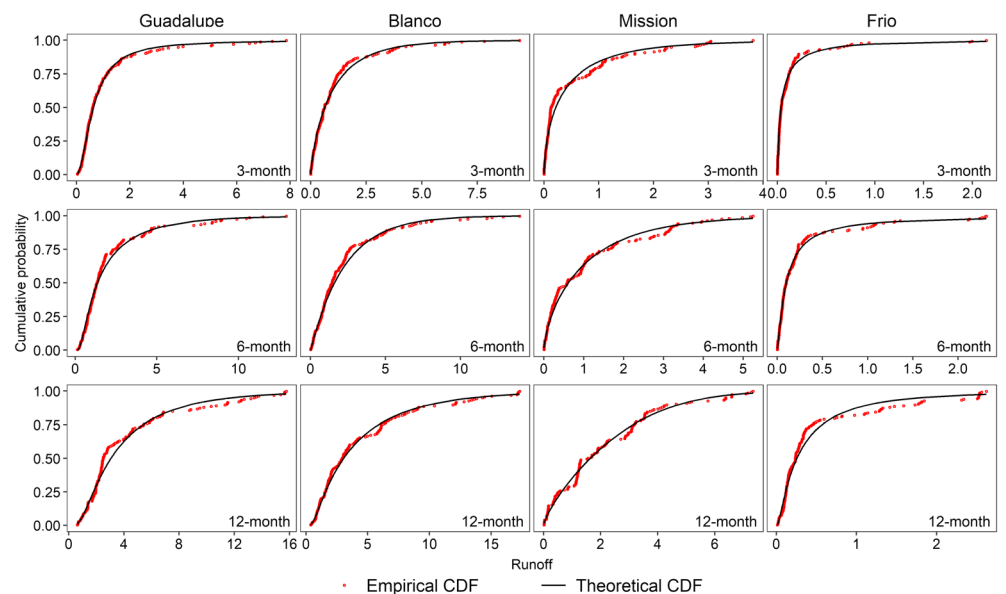


**Figure 5.** Comparison between the empirical CDFs and the theoretical CDFs for 3-, 6-, and 12-month runoff. The red points denote the empirical CDF, while the black lines denote the fitted optimal theoretical CDF. CDF = cumulative distribution function.

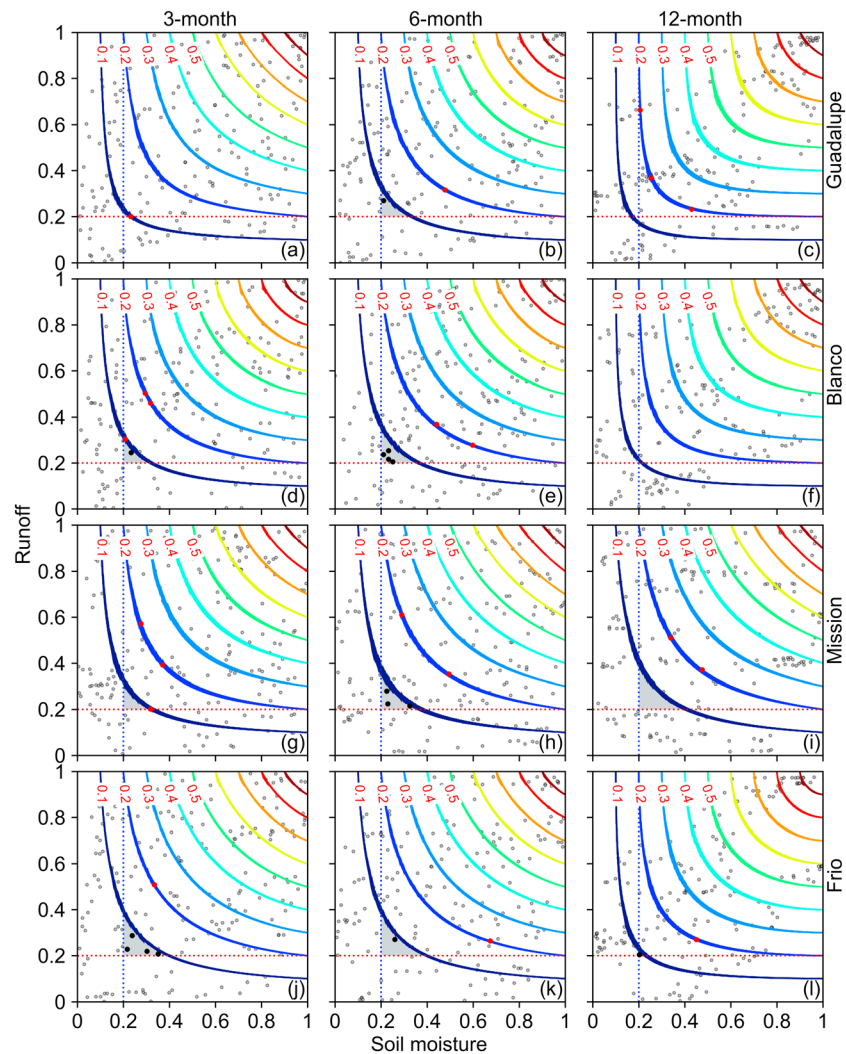


**Figure 6.** The fitted probabilistic contours of joint CDFs of soil moisture and runoff across different temporal scales in the Guadalupe (a–c), Blanco (d–f), Mission (g–i), and Frio (j–l) river basins. The gray points denote the sample pairs of soil moisture and runoff across different temporal scales, while the highlighted black and red points are the critical samples with potential drought risks identified by the PMDI. The gray shaded area denotes critical cases where the univariate CDFs are larger than 0.2 but the joint CDFs are less than 0.1. CDF = cumulative distribution function; PMDI = probabilistic multivariate drought index.

between soil moisture and runoff for all river basins across various temporal scales. For example, Clayton, Gumbel, Frank, and Gumbel are identified as the optimal copula families for modeling the dependence between the 3-month soil moisture and runoff in the Guadalupe, Blanco, Mission, and Frio river basins, respectively. Both the NSE and RMSE values were calculated to determine the optimal copula families. In addition, uncertainties in copula parameters were addressed in this study using the MCMC algorithm, improving the reliability of dependence structures derived by copulas.

Figure 6 depicts the contours of the joint CDFs with uncertainty ranges owing to copula parameter uncertainties. It can be seen that remarkable uncertainties appear in the derived dependence structures, especially for the Mission river basin (see Figures 6g–6i). These joint CDFs with uncertainty ranges lead to probabilistic drought assessment. Such a probabilistic quantification of multivariate drought characteristics improves upon deterministic drought indices by improving drought risk assessment. For example, the red points, as shown in Figure 6, fall within the uncertainty range of the contour line of 0.2 which is the threshold of droughts. These points may be not identified as a drought event using deterministic drought indices, resulting in an underestimation of droughts. In addition, the red points falling within the uncertainty range of the

contour line of 0.1 which is the threshold of severe droughts can be identified as a moderate drought event (higher than 0.1) using deterministic drought indices without taking into account copula parameter uncertainties. On the other hand, the multivariate drought characterization is able to explicitly reveal potential risks of drought assessment. As shown in Figure 6, the gray shaded area represents the risk of severe multivariate droughts with joint CDF lower than 0.1, while the soil moisture and runoff with marginal probability higher than 0.2 are considered to be not dry separately. By comparing the size of the gray shaded area, it can be seen that the joint drought risks at Mission and Frio river basins are relatively high. It is thus necessary to pay close attention to severe multivariate drought events (as highlighted by black points in the gray shaded area) for all river basins across different temporal scales in order to improve the reliability and robustness of drought risk assessment.

### 3.2. Assessment of Multivariate Drought Characteristics

The copula-based PMDI was introduced to conduct probabilistic assessments of multivariate drought characteristics. Figure 7 presents the temporal variations of the derived 3-, 6-, and 12-month PMDI, SSI, and SRI for the Guadalupe, Blanco, Mission, and Frio river basins during 1981–1995. It can be seen that there are considerable discrepancies between the time series derived by SSI and SRI although the general pattern is consistent. For example, the 6-month SSI detects two relatively short-duration drought events while the 6-month SRI identifies a relatively long duration and severe drought event during 1989–1990, as highlighted by the shaded area in Figure 7e. The total number of drought events detected by SSI and SRI is also different. For example, by using the SSI, the number of short-, medium-, and long-term drought events for the Guadalupe river basin is 15, 12, and 8, respectively; however, the number of corresponding drought events identified based on the SRI becomes 7, 4, and 2, respectively. This discrepancy further suggests the necessity of multivariate drought assessments.

Owing to uncertainties in copula parameters, the PMDI is derived with uncertainty intervals, in which the upper and lower bounds of the interval represent the best- and worst-case scenarios of droughts, respectively. The PMDI and especially the worst-case scenario of the PMDI are lower than either of the SSI and SRI values, indicating that the joint drought risk can be amplified while taking into account multivariate assessment of droughts (i.e., the simultaneous occurrence of different types of droughts). For example, for the Guadalupe river basin, the longest short-term drought events based on SSI, SRI, and the worst-case scenario of the PMDI last for 5, 15, and 29 months, respectively. The corresponding average drought severities are 1.5, 2.5, and 5, respectively. This indicates that the severity and intensity of drought events can be amplified based on the introduced PMDI. The amplified effects on drought characteristics can also be found for the Blanco, Mission, and Frio river basins across various temporal scales. The drought characteristics identified by the worst- and best-case PMDI also differ greatly. For example, the shaded area of Figure 7e indicates that the best-case scenario corresponds to two moderate drought events that last 4 and 8 months, respectively. By contrast, the worst-case scenario identifies a long-duration drought event that lasts 21 months. It is thus necessary to take into account different scenarios of droughts in order to conduct a robust drought risk assessment. In addition, the PMDI is able to improve drought risk assessment through alerting water resource managers to possible threats that would be otherwise missed by univariate drought indices. For example, a drought event occurring in the Blanco river basin in 1994 can be captured based on the PMDI, as shown in the shaded area of Figure 7b. However, such a drought episode cannot be detected by SRI and SSI, resulting in an unreliable drought risk assessment. As shown in the shaded area of Figure 7e, the worst-case scenario of the PMDI also detects the drought onset a month ahead of the SSI and SRI values, which provides meaningful insights into drought evolution under the worse-case scenario so that the drought losses can be minimized. A detailed summary of drought characteristics detected by the introduced PMDI, SSI, and SRI is provided in Table S4 of the supporting information.

### 3.3. Evaluation of Convection-Permitting Climate Simulations

To project future changes in multivariate drought characteristics at a high spatial resolution, the convection-permitting WRF climate simulation was conducted in this study to generate the relevant climate variables including temperature, precipitation, soil moisture, and evapotranspiration. Before projecting the future climate information, the performance of the WRF model needs to be evaluated against historical observations. Since all droughts originate from the deficiency of precipitation, the WRF-simulated precipitation was compared with the PRISM data sets.

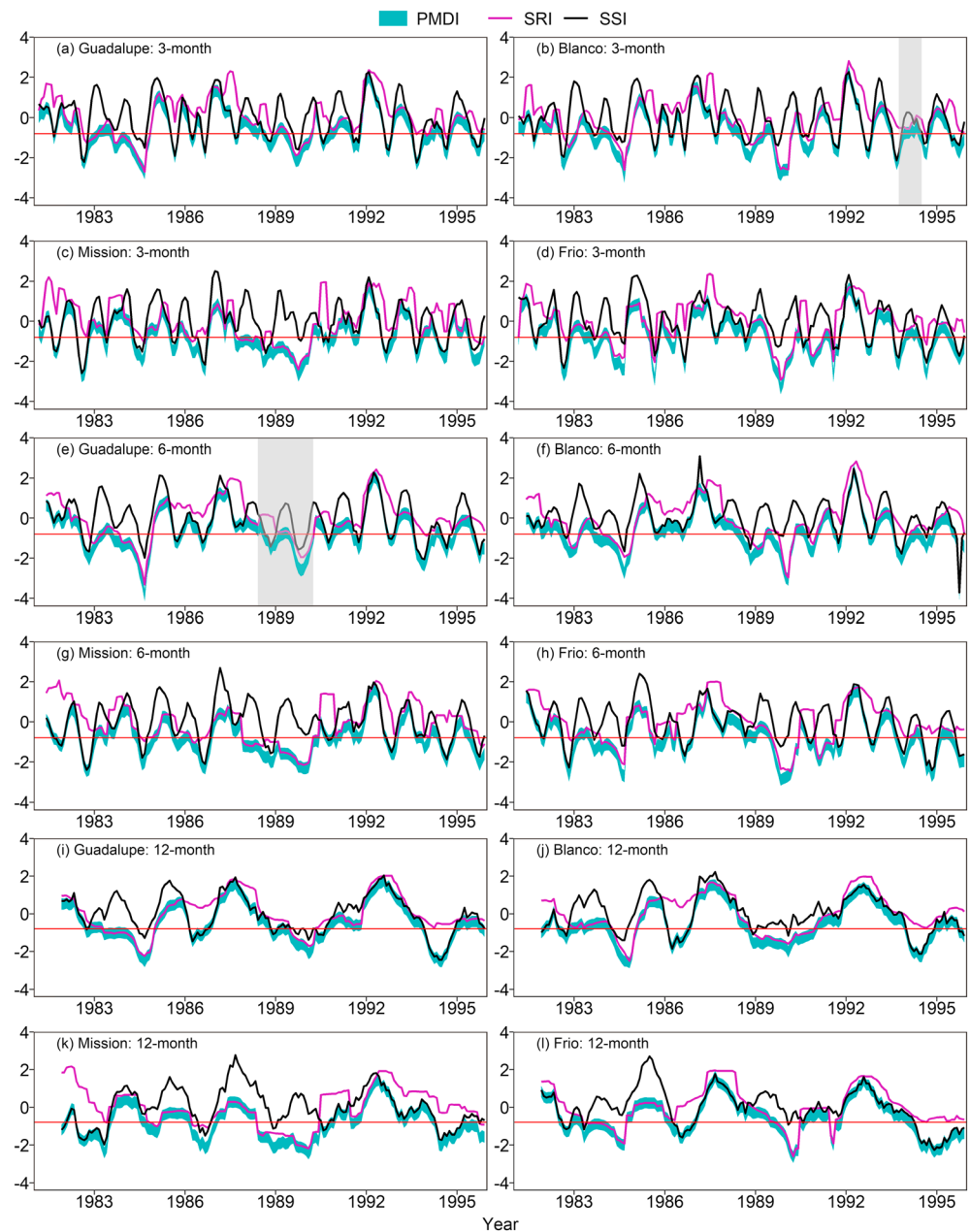


**Figure 7.** Comparison of 3- (a–d), 6- (e–h), and 12-month (i–l) SRI, SSI, and PMDI for the four river basins over South Central Texas. The y axis represents dimensionless values of SRI, SSI, and PMDI. The red horizontal lines denote the drought warning threshold ( $-0.8$ ) in this study. PMDI = probabilistic multivariate drought index; SSI = standardized soil moisture index; SRI = standardized runoff index.

Figure 8 present the spatial distributions of the 15-year seasonal mean precipitation derived from the WRF simulation and the PRISM data sets, as well as their absolute and relative biases in spring (March–April–May, MAM), summer (June–July–August, JJA), fall (September–October–November, SON), and winter (December–January–February, DJF), respectively. In general, the WRF simulation and the PRISM data set show a similar spatial pattern of the seasonal mean precipitation for all seasons. The spatial patterns of absolute and relative differences show a significant seasonal variation. The WRF simulation tends to overpredict the seasonal precipitation for the spring (MAM) and summer (JJA) over the study area. In contrast, the consistency between the WRF-simulated precipitation and the PRISM precipitation is higher in the fall (SON) and



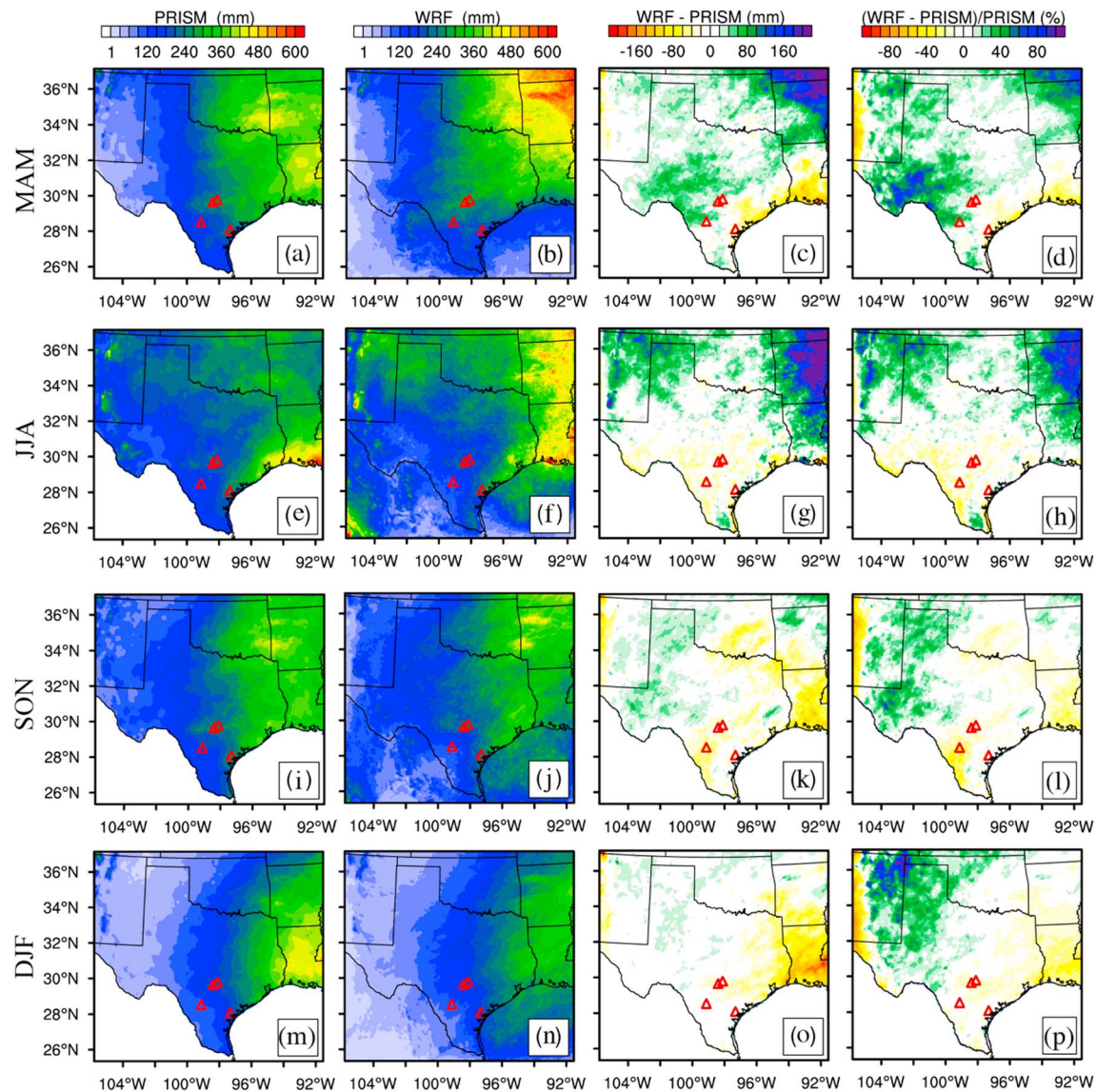


**Figure 8.** Spatial patterns of 15-year seasonal mean precipitation generated from the PRISM observation, the WRF simulation, absolute model bias (WRF-PRISM), and relative model bias. (a–d) MAM, (e–h) JJA, (i–l) SON, and (m–p) DJF. WRF = Weather Research and Forecasting; PRISM = Parameter-elevation Regressions on Independent Slopes Model; SON = September–October–November; MAM = March–April–May; JJA = June–July–August; DJF = December–January–February.

winter (DJF) months. Specifically, the WRF simulation performs well at South Central Texas for all seasons, which is the focus of this study and thus ensures the credibility of simulation results.

In addition to the difference between the WRF-simulated precipitation and the PRISM precipitation, the difference between the CFSR precipitation and the PRISM precipitation for the summer months (JJA) is also examined (see Figure S2 of the supporting information). The difference of the WRF-PRISM summer precipitation is much smaller than that of the CFSR-PRISM summer precipitation, especially for South Central Texas. This indicates that the WRF-simulated precipitation significantly outperforms the CFSR precipitation for the summer months. This is because the convective precipitation is prevalent during the summer season over South Central Texas, which cannot be captured by the coarse-resolution model simulations. The CFSR product with a relatively coarse spatial resolution is thus unable to characterize the detailed spatial variability of the convective precipitation. In comparison, the WRF model enables the kilometer-scale simulation of convective summertime precipitation, well reproducing the historical precipitation pattern and the fine-scale spatial heterogeneity. Since droughts result from a deficiency of precipitation over an extended

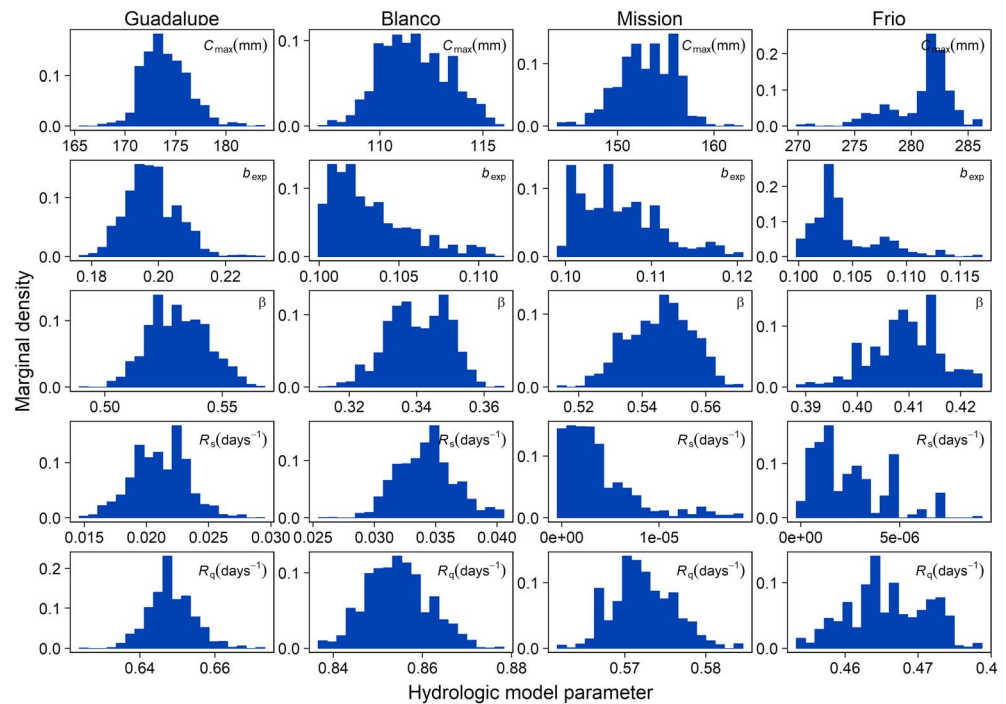


**Figure 9.** Posterior distributions of hydrologic model parameters ( $C_{\max}$ ,  $b_{\exp}$ ,  $\beta$ ,  $R_s$ ,  $R_q$ ) in the Guadalupe, Blanco, Mission, and Frio river basins.

period of time, the accurate simulation of precipitation is crucial to enhancing the reliability of drought risk assessment. In addition, the precipitation is the most important climate variable affecting the hydrological cycle; the reliable projection of high-resolution precipitation information plays a key role in assessing the climate change impacts on future hydrological drought characteristics.

### 3.4. Probabilistic Rainfall-Runoff Predictions

Probabilistic rainfall-runoff simulations were carried out in this study to assess changes in streamflow regimes for the four major river basins in South Central Texas, including Guadalupe, Blanco, Mission, and Frio river basins. The uncertainty in hydrological model parameters was explicitly addressed through the MCMC simulations. Figure 9 depicts the marginal posterior distributions of the five model parameters for the four river basins. To validate the hydrological model, the derived posterior parameter distributions were used to predict daily streamflow time series that can then be compared against the streamflow observations obtained from the MOPEX data set. Figure 10 presents the daily streamflow predictions with the 95% uncertainty range in the calibration period (1981–1990) and the validation period (1991–1995) for the four river basins. It can be seen that a large majority of the predicted streamflow time series match well with the observations although some of high flows cannot be captured due to the deficiency of conceptual hydrological models. Multiple model structures including both conceptual and physically based models will be used in future studies to improve the accuracy of high flow simulations. For the calibration period, 87.51%, 85.08%, 90.12%, and 97.62% of observations fall within the 95% uncertainty range of streamflow predictions for Guadalupe, Blanco, Mission, and Frio river basins, respectively. For the validation period, 87.84%, 84.06%, 85.87%, and 96.88% of observations are captured in the uncertainty range of streamflow predictions. The large proportion of observations captured in the prediction uncertainty range indicates that the hydrological model can be used to characterize the rainfall-runoff process in the four river basins over South Central Texas.

Since precipitation is the most important variable affecting hydrological regimes and drought characteristics, the spatial patterns of 15-year daily mean precipitation for the future climate and the absolute difference between past and future climates are shown in Figure 11. It can be seen that the study domain is dominated by a drying climate except for south Texas and the Gulf of Mexico. The projected daily precipitation can be

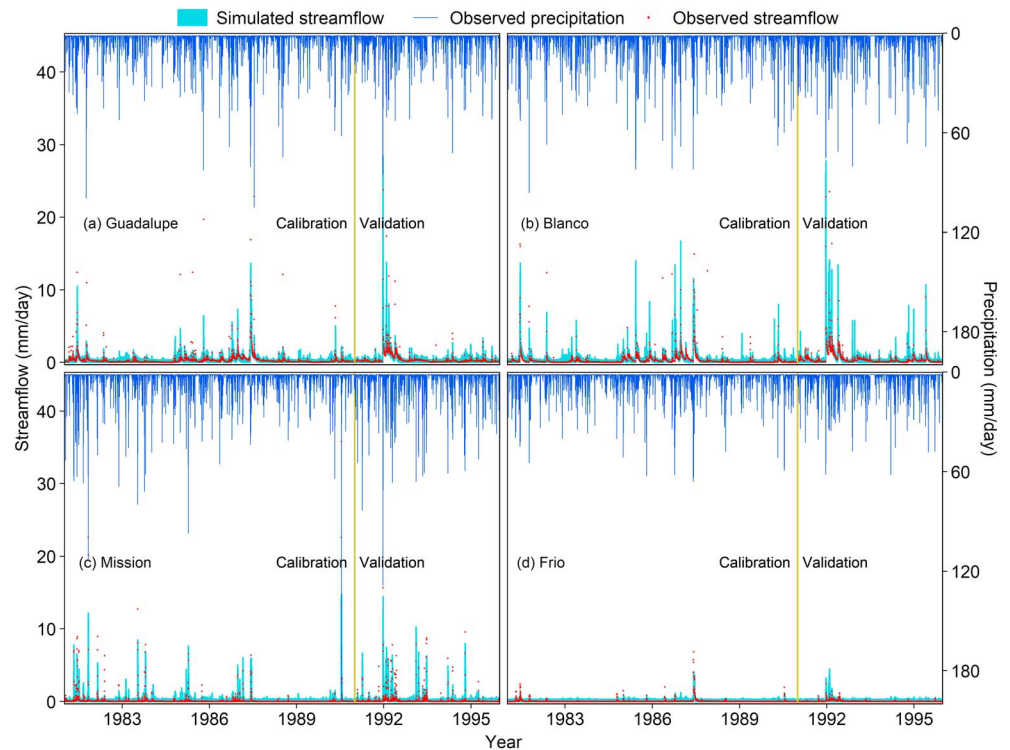


**Figure 10.** Daily rainfall-runoff predictions for the (a) Guadalupe, (b) Blanco, (c) Mission, and (d) Frio river basins over South Central Texas over a period of 15 years (1981–1995). The light blue area represents the predicted streamflow time series with the 95% uncertainty range. Red dots represent streamflow observations. The dark blue line represents precipitation observations.

used to predict future streamflow regimes by using the hydrological model validated against historical observations. Figure 12 presents the probabilistic prediction of future rainfall-runoff time series. Compared with the historical precipitation, the intensity of the future extreme precipitation is expected to increase for the four river basins. Specifically, the total amount of the heaviest rainfall event during 1981–1995 are 98, 90, 187, and 61 mm for Guadalupe, Blanco, Mission, and Frio river basins, respectively; in comparison, the corresponding amounts of future rainfall are projected to increase up to 160, 123, 310, and 255 mm, respectively. Furthermore, the number of future heavy rainfall events with daily precipitation larger than 25 mm is projected to increase by 34%, 12%, 68%, and 49%, respectively. In addition, the number of future dry days with total precipitation less than 1 mm is also projected to increase for the four river basins. Specifically, 75% of

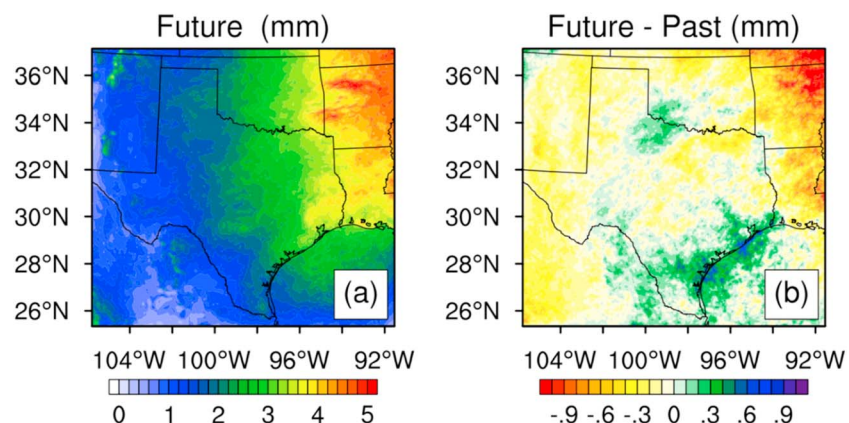


**Figure 11.** Spatial patterns of 15-year daily mean precipitation for (a) the future climate and (b) the absolute difference in precipitation between the past and future climates.



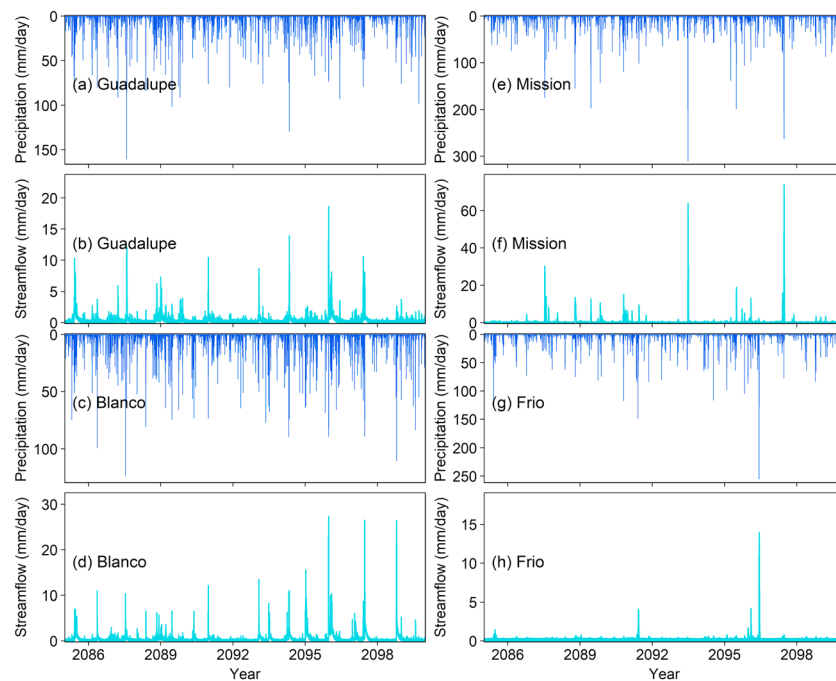


**Figure 12.** Probabilistic daily rainfall-runoff projections for the four major river basins over South Central Texas by the end of the 21st century. The light blue area and the dark blue line represent the projected streamflow and precipitation, respectively. (a and b) Guadalupe, (c and d) Blanco, (e and f) Mission, and (g and h) Frio river basins.

the days are dry for all the four river basins in the past, which are projected to increase up to 83%, 83%, 83%, and 88%. Our findings reveal that the frequency and intensity of extreme precipitation are expected to increase in a changing climate although there will be a reduction in the number of rainfall events over South Central Texas. It should be noted that the future changes in hydroclimatic regimes are projected under RCP8.5, which is the high emissions pathway (emissions are assumed to continue increasing throughout the century). The projected frequency and intensity of extreme events would vary under different emissions pathways. What will be the evolution of future drought characteristics in view of the increasing trend in extreme precipitation under climate change? To answer this question, future changes in multivariate drought characteristics were assessed based on the introduced PMDI.

### 3.5. Projected Changes in Joint Drought Characteristics

The copula-based PMDI was used to assess future changes in multivariate drought characteristics across different temporal scales based on the projected streamflow and soil moisture. Figures 13a–13d present the 3-month PMDI for assessing the short-term drought characteristics in past and future climates for Guadalupe, Blanco, Mission, and Frio river basins, respectively. The worst-case scenario of the PMDI represents the maximum risk of joint droughts including the hydrological drought as a result of the streamflow deficit and the agricultural drought as a result of the deficiency of soil moisture. It provides meaningful insights into the understanding and assessment of joint drought risks, which is crucial to developing a proactive hazard preparedness plan. Thus, the worst-case scenario of the PMDI was used to assess changes in multivariate drought characteristics. It can be seen that the temporal variation of the 3-month PMDI in past and future climates is generally consistent, which is also demonstrated by the similar number of historical and future drought events. Nevertheless, the projected future climate change has a considerable influence on the short-term drought characteristics. Specifically, the short-term drought duration is projected to be greatly shortened by the end of this century. For example, the longest historical drought events for Guadalupe, Blanco, Mission, and Frio river basins last for 29, 25, 31, and 30 months, respectively. By contrast, the maximum duration of future droughts becomes 16, 22, 10, and 10 months, respectively. This indicates that the long-lasting droughts are expected to evolve into a series of the short-duration droughts due to the projected increase in the frequency and intensity of extreme precipitation under climate change. In addition, the

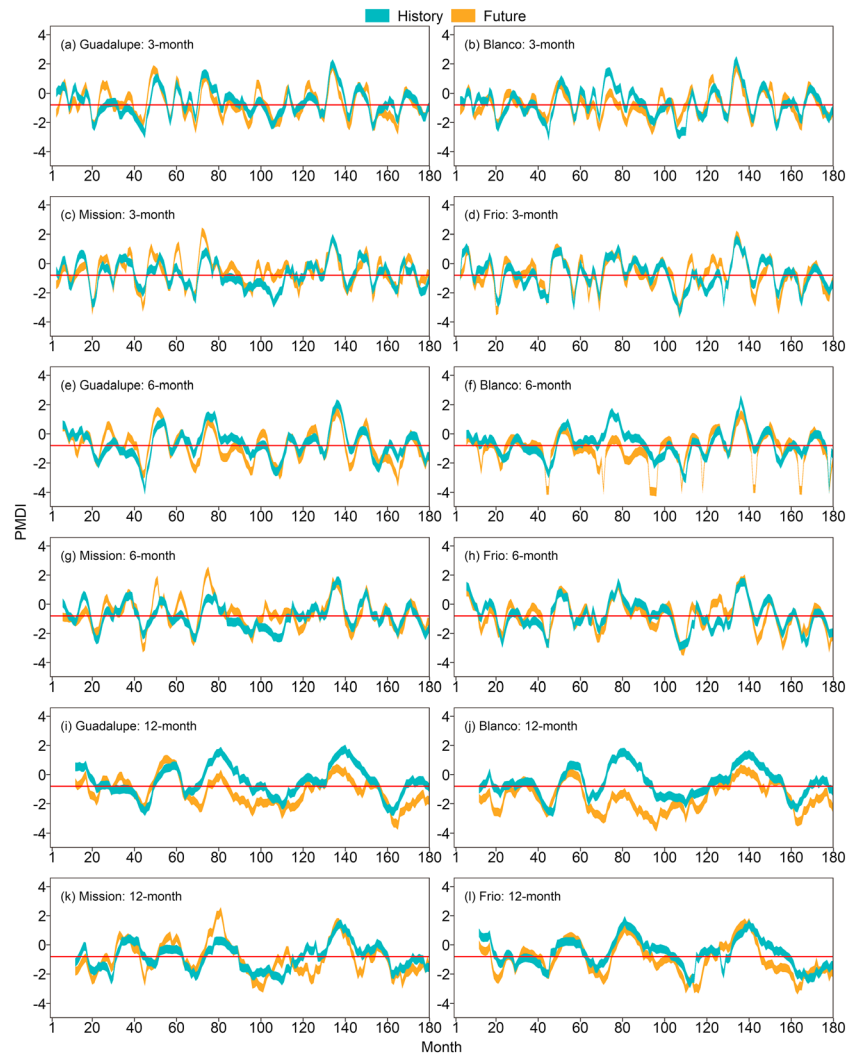


**Figure 13.** Comparison of multivariate drought characteristics in past and future climates based on 3- (a–d), 6- (e–h), and 12-month (i–l) PMDI. The red horizontal lines denote the drought warning threshold used in this study. PMDI = probabilistic multivariate drought index.

average drought intensity is projected to increase by the end of this century. For example, the average intensities of historical droughts for Guadalupe, Blanco, Mission, and Frio river basins are 0.58, 0.65, 0.62, and 0.70, respectively. The corresponding average intensities of future droughts increase up to 0.74, 0.76, 0.70, and 0.75, respectively. This implies that future drought intensities are expected to increase and become consistent for the four river basins over South Central Texas in a changing climate. Nevertheless, it should be noted that the future drought severity is not necessarily projected to increase as a result of the decreasing drought duration for all river basins.

The 6-month PMDI was used to assess climate change impacts on the medium-term droughts. As shown in Figures 13e–13h, the seasonal cycles of the medium-term droughts are consistent for historical and future periods for the four river basins. However, the effects of climate change on the medium-term droughts appear to be more pronounced in comparison with the short-term droughts, especially for the Blanco river basin (see Figure 13f). Although the number of drought events at the Blanco river basin is projected to decrease under climate change, the severity and intensity of future droughts are expected to increase by more than twice by the end of this century. Thus, the Blanco river basin is expected to experience the most significant change in the medium-term drought characteristics (see Table S5 of the supporting information). In addition to the Blanco river basin, the other three river basins are expected to experience an increasing



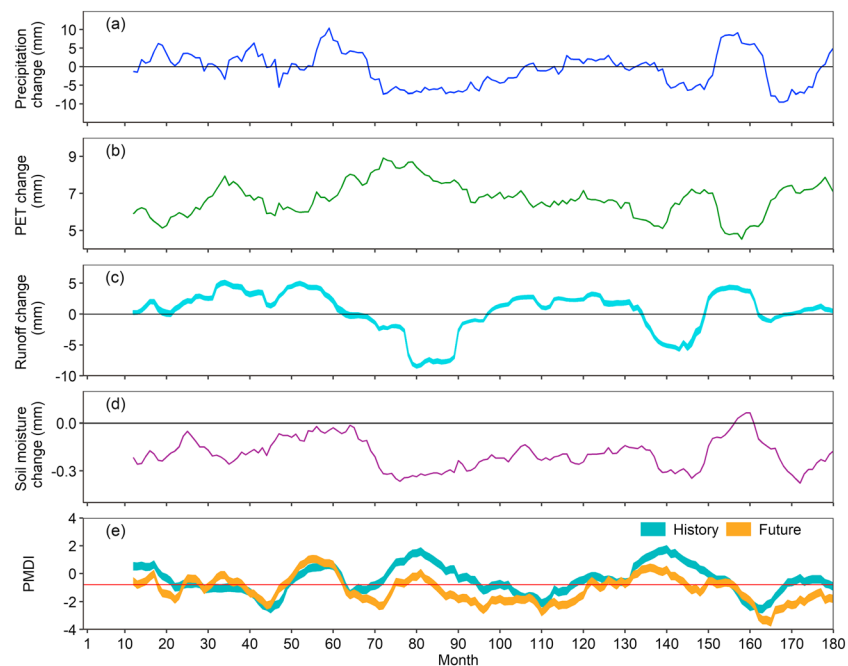


**Figure 14.** Temporal variations in hydrological variables and the 12-month PMDI for historical and future periods in the Guadalupe river basin. (a–e) The temporal variation in the changes of the 12-month precipitation, PET, runoff, and soil moisture as well as PMDI, respectively. PMDI = probabilistic multivariate drought index; PET = potential evapotranspiration.

intensity and a decreasing severity of future medium-term droughts due to the reduction in the drought duration, which is similar to the change in the short-term drought characteristics. Overall, the future medium-term drought events are projected to become shorter and more intense, which provides valuable information and meaningful insights into agricultural management and crop yields in a changing climate.

To examine climate change impacts on the long-term droughts, Figures 13i–13l present the comparison of the 12-month PMDI for historical and future periods. It can be seen that the duration, severity, and intensity of future long-term droughts are projected to increase by the end of this century (see Table S5 of the supporting information). In comparison, the Blanco river basin is expected to experience a significant change in the long-term drought characteristics under climate change. Specifically, although the number of future drought events will decrease for the Blanco river basin, the severity and intensity of droughts are projected to increase by more than 4 times and nearly double, respectively. In general, our findings reveal that climate change impacts on multivariate drought characteristics will intensify with the increasing temporal scales (i.e., short-, medium-, and long-term droughts) although the number of future drought events may decrease by the end of this century. The high-resolution projection of future changes in multivariate drought characteristics plays a crucial role in strengthening resilience to the climate-induced drought hazard for facilitating sustainable agricultural development and water resources planning in a changing climate.

The projected changes in joint drought characteristics present a paradox that droughts are projected to be more severe while precipitation is expected to become more intense in a changing climate. To address the paradox, it is necessary to reveal whether soil moisture or runoff plays the dominant role in causing the severe joint droughts. Thus, we further investigated the changes of hydroclimatic variables (precipitation, PET, runoff, and soil moisture) and their potential influence on joint drought characteristics. Figures 14a–14b present the changes of precipitation and PET at a 12-month temporal scale for the Guadalupe river basin. Although the extreme precipitation is projected to increase (Figure 12a), there will be a considerable decrease in the 12-month precipitation. The pattern of the 12-month precipitation change is consistent to the runoff pattern (Figure 14c) because precipitation is the most dominant climatic factor affecting the runoff process. By contrast, the PET is projected to increase significantly, resulting in a considerable reduction in soil moisture (Figure 14d). Consequently, the projected decrease in both soil moisture and runoff results

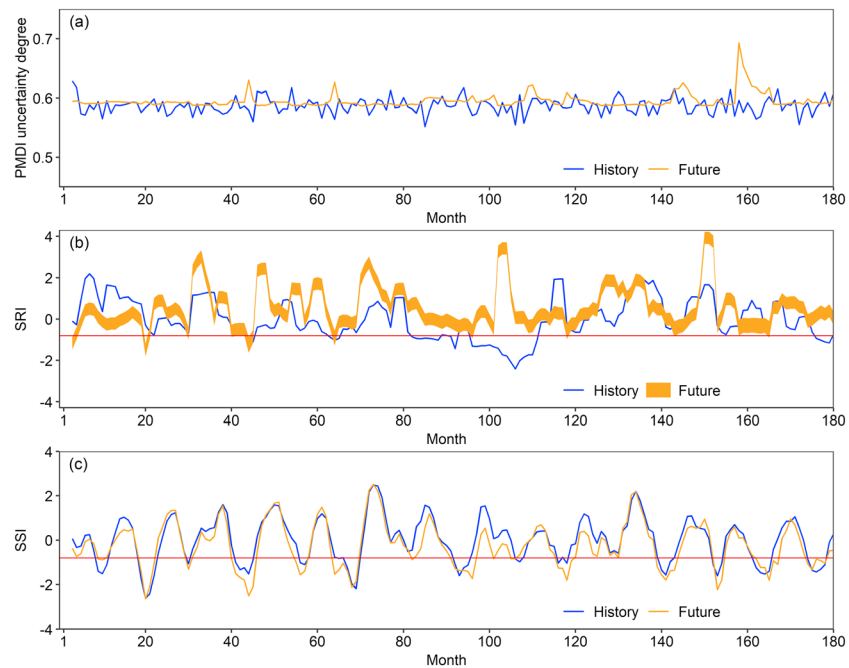


**Figure 15.** Assessment of uncertainty in the 3-month PMDI for the Mission river basin. (a) Temporal variation in degrees of the PMDI uncertainty for historical and future periods. (b) Time series of the 3-month SRI for historical and future periods. (c) Time series of the 3-month SSI for historical and future periods. PMDI = probabilistic multivariate drought index; SSI = standardized soil moisture index; SRI = standardized runoff index.

in more severe droughts (Figure 14e). Although the extreme precipitation is projected to increase, more rain can be absorbed by the drier soils that reduce the volume of runoff. Furthermore, the rising temperature intensifies the soil water evaporation, further accelerating the drying of soils. As a result, droughts are expected to become more severe and intense in a changing climate. It should be also noted that the future changes in multivariate drought characteristics are projected under RCP8.5, which is the high emissions pathway (emissions are assumed to continue increasing throughout the century). The projected frequency, intensity, and severity of droughts therefore vary under different emissions pathways.

### 3.6. Uncertainty Assessment of Multivariate Drought Projections

Since uncertainties in copula parameters and hydrologic predictions were addressed and propagated into probabilistic drought projections, it is necessary to quantify the contribution of different sources of uncertainty in order to advance our understanding in the copula-based probabilistic projection of multivariate drought characteristics. Figure 15a presents the temporal variation in the uncertainty degree (i.e., difference between the worst- and best-case PMDI) of the 3-month PMDI for the Mission river basin as an illustrative example. It can be seen that the degree of uncertainty remains stable at around 0.6 for both the historical period without the consideration of uncertainty in hydrologic predictions and the future period with the consideration of uncertainty in hydrologic predictions. This implies that the overall uncertainty in multivariate drought projections is mainly attributed to copula parameters instead of hydrologic predictions. To further explore different sources of uncertainty, Figures 15b–15c show the 3-month SRI and SSI for the Mission river basin. The future SRI is depicted with an uncertainty range due to the consideration of uncertainty in hydrologic predictions. It can be seen that there is an increase in the degree of the PMDI uncertainty (Figure 15a) when a hydrological drought event occurs (Figure 15b). By contrast, there is little variation in the degree of the PMDI uncertainty when the agricultural drought event occurs as a result of the deficiency of soil moisture (Figure 15c). Our findings reveal that the uncertainty in hydrologic predictions contributes to the overall uncertainty in multivariate drought projections only when the hydrological drought event occurs. Otherwise, the uncertainty in hydrologic predictions can be neglected in comparison with the uncertainty in copula parameters for probabilistic drought projections.

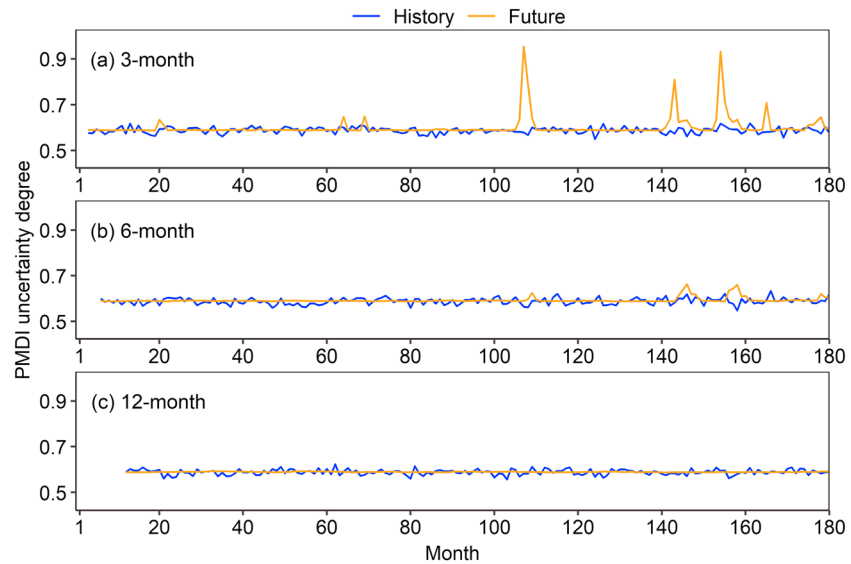


**Figure 16.** Temporal variation in the degrees of the PMDI uncertainty in the 3- (a), 6- (b), and 12-month (c) PMDI for the Frio river basin during historical and future periods. PMDI = probabilistic multivariate drought index.

To assess the change in the degree of the PMDI uncertainty across different temporal scales, Figure 16 presents the temporal variation in the degree of uncertainty of the 3-, 6-, and 12-month PMDI for the Frio river basin as an illustrative example. The pattern of the PMDI uncertainty appears to be similar for the historical period across all temporal scales, whereas the degree of the PMDI uncertainty becomes more stable with increasing temporal scales. This implies that the contribution of the uncertainty in hydrological drought predictions to the overall PMDI uncertainty decreases with the increasing temporal scales. These findings are useful for advancing our understanding of different sources of uncertainty inherent in probabilistic projections of multivariate drought characteristics.

#### 4. Summary and Conclusions

In this study, we develop the copula-based high-resolution probabilistic projections of future changes in multivariate drought characteristics, in which a PMDI is introduced to examine the joint effects of the soil moisture deficit (agricultural drought) and the runoff deficit (hydrological drought) across different temporal scales. The high-resolution climate projections were developed using the convection-permitting WRF model with the 4-km horizontal grid spacing, and then the probabilistic streamflow predictions were carried out for four major river basins over South Central Texas through the MCMC simulations based on the WRF-derived climate information. Furthermore, the copula-based PMDI was used to characterize future changes in multivariate characteristics of short-, medium, and long-term droughts. In addition, the contributions of different sources of uncertainty, including uncertainties in hydrologic predictions and in copula parameters, to the overall PMDI uncertainty were examined for probabilistic drought projections.

The introduced copula-based PMDI improves upon the univariate drought indices not only by taking into account the joint assessment of droughts (i.e., the simultaneous occurrence of different types of droughts) but also by addressing best- and worse-case scenarios of droughts resulting from uncertainties inherent in multivariate drought characterization. Our findings indicate that the PMDI can be used to improve drought risk assessment through detecting potential threats that would be otherwise missed by univariate drought indices. Furthermore, the severity and intensity of drought events can be amplified based on the PMDI across different temporal scales. It is thus necessary to conduct probabilistic quantification of multivariate drought characteristics in order to improve the reliability and robustness of drought risk assessment. The convection-permitting climate simulations well reproduce historical climate variables through comparison against CFSR and PRISM data sets, especially for the summertime precipitation over South Central Texas which is the focused region of this study. This indicates that the convection-permitting climate

simulations are able to characterize convective summertime precipitation with kilometer-scale spatial heterogeneity that cannot be captured by coarse-resolution model simulations. Since droughts originate from the deficiency of precipitation, the accurate simulation of precipitation is crucial to enhancing the reliability of drought risk assessment.

The projected future changes in multivariate drought characteristics indicate that the long-lasting droughts are expected to evolve into a series of short-duration droughts due to the projected increase in the frequency and intensity of extreme precipitation in a changing climate. In addition, the average drought intensity is projected to increase and become consistent for the four major river basins over South Central Texas, whereas the severity of droughts is not necessarily projected to increase as a result of the decreasing drought duration. Moreover, our findings reveal that climate change impacts on multivariate drought characteristics will intensify with the increasing temporal scales (i.e., short-, medium-, and long-term droughts), although the number of future drought events may decrease by the end of this century. The high-resolution projection of future changes in multivariate drought characteristics across different temporal scales plays a crucial role in strengthening resilience to the climate-induced drought hazard and in facilitating sustainable agricultural development and water resources planning in a changing climate. In addition, our findings indicate that the uncertainty in copula parameters plays a dominant role in contributing to the overall uncertainty in probabilistic drought projections. In comparison, the contribution of the uncertainty in hydrologic predictions to the overall uncertainty appears to be less significant and even decreases with the increasing temporal scales. These findings are useful for advancing our understanding of different sources of uncertainty inherent in probabilistic projections of multivariate drought characteristics.

It should be noted that the probabilistic prediction of future streamflow time series was carried out in this study through the MCMC simulations based on a conceptual rainfall-runoff model that cannot well represent spatial heterogeneity of river basins. Although a large proportion of observations can be captured in the prediction uncertainty range, it is desired to further improve the accuracy of streamflow simulations using physically based hydrologic models in future studies. In addition, the convection-permitting climate projections were conducted for a 15-year future period which may not be long enough to well characterize the long-term drought characteristics. It is thus necessary to develop convection-permitting climate simulations for a long period of time (more than 30 years) when the computational resources are available.

## Acknowledgments

This research was supported by the National Natural Science Foundation of China (grant 51809223) and the Hong Kong Polytechnic University Start-up Grant (grant 1-ZE8S). The daily hydrological data for Guadalupe, Blanco, Mission, and Frio river basins were collected from the U.S. MOPEX data set. The PRISM data set was provided by the NOAA/OAR/ESRL PSD, Boulder, Colorado, USA. The CFSR data set was developed by NOAA's National Centers for Environmental Prediction (NCEP). We acknowledge the World Climate Research Programme's Working Group on Coupled Modeling, which is responsible for CMIP5, and we thank the climate modeling groups for producing and making their model outputs available. We would also like to express our sincere gratitude to the Editor and anonymous reviewers for their constructive comments and suggestions.

## References

- AghaKouchak, A. (2014). A baseline probabilistic drought forecasting framework using standardized soil moisture index: Application to the 2012 United States drought. *Hydrology and Earth System Sciences*, 18(7), 2485–2492. <https://doi.org/10.5194/hess-18-2485-2014>
- AghaKouchak, A., Cheng, L., Mazdiyasni, O., & Farahmand, A. (2014). Global warming and changes in risk of concurrent climate extremes: Insights from the 2014 California drought. *Geophysical Research Letters*, 41, 8847–8852. <https://doi.org/10.1002/2014GL062308>
- Allen, R. G., Pereira, L. S., Raes, D., & Smith, M. (1998). Crop evapotranspiration—Guidelines for computing crop water requirements – FAO Irrigation and drainage paper 56. *Fao, Rome*, 300(9), D05109.
- Berg, P., Wagner, S., Kunstmann, H., & Schädler, G. (2013). High resolution regional climate model simulations for Germany: Part I – validation. *Climate Dynamics*, 40(1–2), 401–414. <https://doi.org/10.1007/s00382-012-1508-8>
- Brockhaus, P., Lüthi, D., & Schär, C. (2008). Aspects of the diurnal cycle in a regional climate model. *Meteorologische Zeitschrift*, 17(4), 433–443. <https://doi.org/10.1127/0941-2948/2008/0316>
- Carvalho, K. S., & Wang, S. (2019). Characterizing the Indian Ocean sea level changes and potential coastal flooding impacts under global warming. *Journal of Hydrology*, 569, 373–386. <https://doi.org/10.1016/j.jhydrol.2018.11.072>
- Genest, C., Rémillard, B., & Beaudoin, D. (2009). Goodness-of-fit tests for copulas: A review and a power study. *Insurance: Mathematics & Economics*, 44(2), 199–213. <https://doi.org/10.1016/j.insmatheco.2007.10.005>
- Hao, Z., & AghaKouchak, A. (2013). Multivariate standardized drought index: A parametric multi-index model. *Advances in Water Resources*, 57, 12–18. <https://doi.org/10.1016/j.advwatres.2013.03.009>
- Herman, J. D., Reed, P. M., & Wagener, T. (2013). Time-varying sensitivity analysis clarifies the effects of watershed model formulation on model behavior. *Water Resources Research*, 49, 1400–1414. <https://doi.org/10.1002/wrcr.20124>
- Huang, S., Chang, J., Leng, G., & Huang, Q. (2015). Integrated index for drought assessment based on variable fuzzy set theory: A case study in the Yellow River basin, China. *Journal of Hydrology*, 527, 608–618. <https://doi.org/10.1016/j.jhydrol.2015.05.032>
- Johnson, F., & Sharma, A. (2015). What are the impacts of bias correction on future drought projections? *Journal of Hydrology*, 525, 472–485. <https://doi.org/10.1016/j.jhydrol.2015.04.002>
- Kang, H., & Sridhar, V. (2017). Combined statistical and spatially distributed hydrological model for evaluating future drought indices in Virginia. *Journal of Hydrology: Regional Studies*, 12, 253–272. <https://doi.org/10.1016/j.ejrh.2017.06.003>
- Kao, S. C., & Govindaraju, R. S. (2010). A copula-based joint deficit index for droughts. *Journal of Hydrology*, 380(1–2), 121–134. <https://doi.org/10.1016/j.jhydrol.2009.10.029>
- Keyantash, J. A., & Dracup, J. A. (2004). An aggregate drought index: Assessing drought severity based on fluctuations in the hydrologic cycle and surface water storage. *Water Resources Research*, 40, W09304. <https://doi.org/10.1029/2003WR002610>

- Kwon, H., & Lall, U. (2016). A copula-based nonstationary frequency analysis for the 2012–2015 drought in California. *Water Resources Research*, 52, 5662–5675. <https://doi.org/10.1002/2016WR018959>
- Lauer, A., Zhang, C., Elison-Timm, O., Wang, Y., & Hamilton, K. (2013). Downscaling of climate change in the hawaii region using CMIP5 results: On the choice of the forcing fields\*. *Journal of Climate*, 26(24), 10,006–10,030. <https://doi.org/10.1175/JCLI-D-13-00126.1>
- Leng, G., Tang, Q., & Rayburg, S. (2015). Climate change impacts on meteorological, agricultural and hydrological droughts in China. *Global and Planetary Change*, 126, 23–34. <https://doi.org/10.1016/j.gloplacha.2015.01.003>
- Liu, C., Ikeda, K., Rasmussen, R., Barlage, M., Newman, A. J., Prein, A. F., et al. (2017). Continental-scale convection-permitting modeling of the current and future climate of North America. *Climate Dynamics*, 49(1–2), 71–95. <https://doi.org/10.1007/s00382-016-3327-9>
- McKee, T. B., Doesken, N. J., & Kleist, J. (1993). The relationship of drought frequency and duration to time scales. In *Proceedings of the 8th Conference on Applied Climatology* (Vol. 17, pp. 179–183). MA: American Meteorological Society Boston.
- Mo, K. C. (2008). Model-based drought indices over the United States. *Journal of Hydrometeorology*, 9(6), 1212–1230. <https://doi.org/10.1175/2008JHM1002.1>
- Moon, H., Gudmundsson, L., & Seneviratne, S. I. (2018). Drought persistence errors in global climate models. *Journal of Geophysical Research: Atmospheres*, 123, 3483–3496. <https://doi.org/10.1002/2017JD027577>
- Moore, R. J. (1985). The probability-distributed principle and runoff production at point and basin scales. *Hydrological Sciences Journal*, 30(2), 273–297. <https://doi.org/10.1080/02626668509490989>
- Moore, R. J. (2007). The PDM rainfall-runoff model. *Hydrology and Earth System Sciences*, 11(1), 483–499. <https://doi.org/10.5194/hess-11-483-2007>
- Pozzi, W., Sheffield, J., Stefanski, R., Cripe, D., Pulwarty, R., Vogt, J. V., et al. (2013). Toward global drought early warning capability: Expanding international cooperation for the development of a framework for monitoring and forecasting. *Bulletin of the American Meteorological Society*, 94(6), 776–785. <https://doi.org/10.1175/BAMS-D-11-00176.1>
- Prein, A. F., Gobiet, A., Suklitsch, M., Truhetz, H., Awan, N. K., Keuler, K., & Georgievski, G. (2013). Added value of convection permitting seasonal simulations. *Climate Dynamics*, 41(9–10), 2655–2677. <https://doi.org/10.1007/s00382-013-1744-6>
- Prudhomme, C., Giuntoli, I., Robinson, E. L., Clark, D. B., Arnell, N. W., Dankers, R., et al. (2014). Hydrological droughts in the 21st century, hotspots and uncertainties from a global multimodel ensemble experiment. *Proceedings of the National Academy of Sciences*, 111(9), 3262–3267. <https://doi.org/10.1073/pnas.1222473110>
- Rad, A. M., Ghahraman, B., Khalili, D., Ghahremani, Z., & Ardakani, S. A. (2017). Integrated meteorological and hydrological drought model: A management tool for proactive water resources planning of semi-arid regions. *Advances in Water Resources*, 107, 336–353. <https://doi.org/10.1016/j.advwatres.2017.07.007>
- Rajsekhar, D., & Gorelick, S. M. (2017). Increasing drought in Jordan: Climate change and cascading Syrian land-use impacts on reducing transboundary flow. *Science Advances*, 3(8), 1–16. <https://doi.org/10.1126/sciadv.1700581>
- Rajsekhar, D., Singh, V. P., & Mishra, A. K. (2015a). Integrated drought causality, hazard, and vulnerability assessment for future socioeconomic scenarios: An information theory perspective. *Journal of Geophysical Research: Atmospheres*, 120, 6346–6378. <https://doi.org/10.1002/2014JD022670>
- Rajsekhar, D., Singh, V. P., & Mishra, A. K. (2015b). Multivariate drought index: An information theory based approach for integrated drought assessment. *Journal of Hydrology*, 526, 164–182. <https://doi.org/10.1016/j.jhydrol.2014.11.031>
- Roy, T., Serrat-Capdevila, A., Gupta, H., & Valdes, J. (2017). A platform for probabilistic multimodel and multiproduct streamflow forecasting. *Water Resources Research*, 53, 376–399. <https://doi.org/10.1002/2016WR019752>
- Ruosteenoja, K., Markkanen, T., Venäläinen, A., Räisänen, P., & Peltola, H. (2018). Seasonal soil moisture and drought occurrence in Europe in CMIP5 projections for the 21st century. *Climate Dynamics*, 50(3–4), 1177–1192. <https://doi.org/10.1007/s00382-017-3671-4>
- Russo, S., Dosio, A., Sterl, A., Barbosa, P., & Vogt, J. (2013). Projection of occurrence of extreme dry-wet years and seasons in Europe with stationary and nonstationary standardized precipitation indices. *Journal of Geophysical Research: Atmospheres*, 118, 7628–7639. <https://doi.org/10.1002/jgrd.50571>
- Sadeh, M., Ragno, E., & AghaKouchak, A. (2017). Multivariate Copula Analysis Toolbox (MvCAT): Describing dependence and underlying uncertainty using a Bayesian framework. *Water Resources Research*, 53, 5166–5183. <https://doi.org/10.1002/2016WR020242>
- Sadeh, M., & Vrugt, J. A. (2013). Bridging the gap between GLUE and formal statistical approaches: Approximate Bayesian computation. *Hydrology and Earth System Sciences*, 17(12), 4831–4850. <https://doi.org/10.5194/hess-17-4831-2013>
- Su, B., Huang, J., Fischer, T., Wang, Y., Kundzewicz, Z. W., Zhai, J., et al. (2018). Drought losses in China might double between the 1.5 °C and 2.0 °C warming. *Proceedings of the National Academy of Sciences*, 115(42), 201802129. <https://doi.org/10.1073/pnas.1802129115>
- Van Huijgevoort, M. H. J., Van Lanen, H. A. J., Teuling, A. J., & Uijlenhoet, R. (2014). Identification of changes in hydrological drought characteristics from a multi-GCM driven ensemble constrained by observed discharge. *Journal of Hydrology*, 512, 421–434. <https://doi.org/10.1016/j.jhydrol.2014.02.060>
- Vrugt, J. A. (2016). Markov chain Monte Carlo simulation using the DREAM software package: Theory, concepts, and MATLAB implementation. *Environmental Modelling and Software*, 75, 273–316. <https://doi.org/10.1016/j.envsoft.2015.08.013>
- Vrugt, J. A., ter Braak, C. J. F., Clark, M. P., Hyman, J. M., & Robinson, B. A. (2008). Treatment of input uncertainty in hydrologic modeling: Doing hydrology backward with Markov chain Monte Carlo simulation. *Water Resources Research*, 44, W00B09. <https://doi.org/10.1029/2007WR006720>
- Wan, W., Zhao, J., Li, H. Y., Mishra, A., Ruby Leung, L., Hejazi, M., et al. (2017). Hydrological drought in the Anthropocene: Impacts of local water extraction and reservoir regulation in the U.S. *Journal of Geophysical Research: Atmospheres*, 122, 11,313–11,328. <https://doi.org/10.1002/2017JD026899>
- Wang, D., Hejazi, M., Cai, X., & Valocchi, A. J. (2011). Climate change impact on meteorological, agricultural, and hydrological drought in central Illinois. *Water Resources Research*, 47, W09527. <https://doi.org/10.1029/2010WR009845>
- Wang, S., Ancell, B. C., Huang, G. H., & Baetz, B. W. (2018). Improving robustness of hydrologic ensemble predictions through probabilistic pre- and post-processing in sequential data assimilation. *Water Resources Research*, 54, 2129–2151. <https://doi.org/10.1002/2018WR022546>
- Wang, S., Huang, G. H., Baetz, B. W., & Huang, W. (2015). A polynomial chaos ensemble hydrologic prediction system for efficient parameter inference and robust uncertainty assessment. *Journal of Hydrology*, 530, 716–733. <https://doi.org/10.1016/j.jhydrol.2015.10.021>
- Wang, S., & Wang, Y. (2019). Improving probabilistic hydroclimatic projections through high-resolution convection-permitting climate modeling and Markov chain Monte Carlo simulations. *Climate Dynamics*. <https://doi.org/10.1007/s00382-019-04702-7>
- Wehner, M., Easterling, D. R., Lawrimore, J. H., Heim, R. R., Vose, R. S., & Santer, B. D. (2011). Projections of future drought in the continental United States and Mexico. *Journal of Hydrometeorology*, 12(6), 1359–1377. <https://doi.org/10.1175/2011JHM1351.1>



- Xia, Y., Ek, M. B., Peters-Lidard, C. D., Mocko, D., Svoboda, M., Sheffield, J., & Wood, E. F. (2014). Application of USDM statistics in NLDAS-2: Optimal blended NLDAS drought index over the continental United States. *Journal of Geophysical Research: Atmospheres*, 119, 2947–2965. <https://doi.org/10.1002/2013JD020994>
- Yevjevich, V. M. (1967). An objective approach to definitions and investigations of continental hydrologic droughts. *Hydrology Papers (Colorado State University)*; No. 23.
- Zarch, M. A. A., Sivakumar, B., & Sharma, A. (2015). Droughts in a warming climate: A global assessment of standardized precipitation index (SPI) and reconnaissance drought index (RDI). *Journal of Hydrology*, 526, 183–195. <https://doi.org/10.1016/j.jhydrol.2014.09.071>
- Zhu, J., Huang, G., Wang, X., Cheng, G., & Wu, Y. (2018). High-resolution projections of mean and extreme precipitations over China through PRECIS under RCPs. *Climate Dynamics*, 50(11–12), 4037–4060. <https://doi.org/10.1007/s00382-017-3860-1>
- Zhu, J., Wang, S., & Huang, G. (2019). Assessing climate change impacts on human-perceived temperature extremes and underlying uncertainties. *Journal of Geophysical Research: Atmospheres*, 124, 3800–3821. <https://doi.org/10.1029/2018JD029444>